

Approximation properties of multi-patch C^1 isogeometric spaces

Annabelle Collin^a, Giancarlo Sangalli^{a,b}, Thomas Takacs^a

^a*Dipartimento di Matematica “F. Casorati”, Università degli Studi di Pavia, Italy*

^b*Istituto di Matematica Applicata e Tecnologie Informatiche “E. Magenes” (CNR), Italy*

Abstract

One key feature of isogeometric analysis is that it allows smooth shape functions. This is achieved by p -degree splines (and extensions, such as NURBS) that are globally up to C^{p-1} -continuous in each patch. However, global continuity beyond C^0 on so-called multi-patch geometries poses some significant difficulties. In this work, we consider multi-patch domains that have a parametrization which is only C^0 at the patch interface. On such domains we study the h -refinement of C^1 -continuous isogeometric spaces. These spaces in general do not have optimal approximation properties. The reason is that the C^1 -continuity condition easily over-constrains the solution which is, in the worst cases, fully *locked* to linears at the patch interface. However, recently [20] has given numerical evidence that optimal convergence occurs for bilinear two-patch geometries and C^1 splines of polynomial degree at least 3. This is a key result and the starting point of our study. We introduce analysis-suitable G^1 -continuous geometry parametrizations, a class of parametrizations that includes bilinears. We analyze the structure of C^1 isogeometric spaces and, by theoretical results and numerical testing, infer that analysis-suitable G^1 geometry parametrizations are the ones that allow optimal convergence of C^1 isogeometric spaces (under conditions on the continuity along the interface). Beyond analysis-suitable G^1 parametrizations optimal convergence is prevented.

1. Introduction

Thanks to the use of smooth B-splines and NURBS, isogeometric methods [17, 12] have revitalized the interest for the use of smooth approximating functions for the numerical solution of partial differential equations. Advantages with respect to C^0 finite element methods are improved accuracy and spectral properties [13, 4, 18, 32] and the possibility to directly discretize differential operators of order higher than 2. In the literature there are indeed many examples of isogeometric methods for 4th order differential problems of relevant interest, such as Kirchhoff-Love plates/shells [21, 7, 3], the Cahn-Hilliard equation [14], and the Navier-Stokes-Korteweg equation [15].

Since higher dimensional spline spaces possess a tensor-product structure, the representation of domains that have a complex geometry is non-trivial. In this paper we focus on multi-patch representations. While the implementation of C^0 -continuity over multi-patch domains is well understood (see e.g. [22, 5, 30] for strong and [9] for weak imposition of the C^0 conditions), C^1 -continuity is not. Several studies have tackled the problem of constructing function spaces of C^1 or higher order smoothness, such as [10, 19] for spline spaces, [31, 24] for triangulations and [25] comparing both.

Nevertheless, the construction of smooth isogeometric spaces with optimal approximation properties on complex geometries is still an open and challenging problem. This is related to the problem of finding parametrizations of smooth surfaces having complex topology, which is a fundamental area of research in the community of Computer Aided Geometric Design (CAGD) over the last decades.

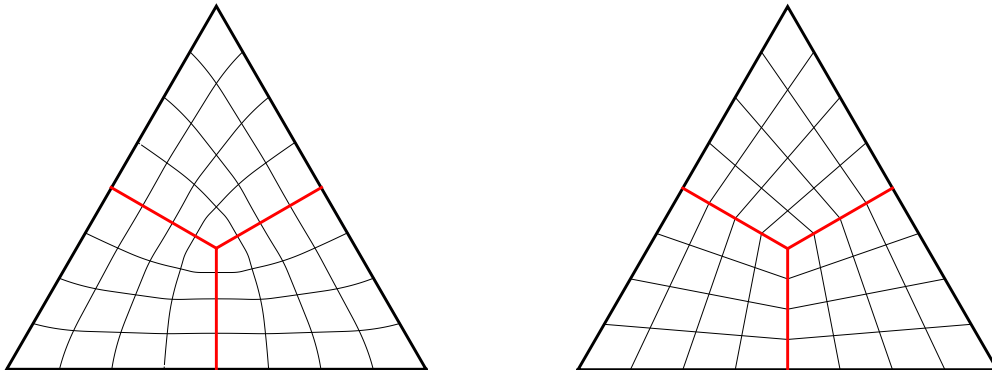


Figure 1: Two possible parametrization schemes: C^1 away from extraordinary points (left) and C^0 everywhere (right).

We review two different strategies for constructing smooth multi-patch geometries and corresponding isogeometric spaces. One possibility is to adopt a geometry parametrization which is globally smooth almost everywhere, with the exception of a neighborhood of the extraordinary points (or edges in 3D), see Figure 1 (left). The other possibility is to use geometry parametrizations that are only C^0 at patch interfaces, see Figure 1 (right). The first option includes subdivision surfaces [11] and the T-spline construction in [29] and, while possessing attractive features, they seem to lack optimal accuracy [25, 19]. In our work we consider the second possibility, corresponding to the right part of Figure 1. The construction of C^1 isogeometric functions over a C^0 parametrization can be interpreted conveniently as geometric continuity G^1 of the graph parametrization. Following this approach, [20] constructed a basis for the shape functions, then analyzed its dimensionality of some configurations and numerically tested the order of convergence on h -refined meshes, obtaining optimal convergence with spline degree 3 or higher and global continuity C^1 on a two-patch bilinear geometry. The authors also show an example of *over-constrained* C^1 isogeometric spaces on a non-bilinear geometry. We refer to the latter situation as C^1 *locking*. Bilinear parametrizations of a multi-patch planar domain have been analyzed in [8], where it was shown that there exists a minimal determining set with local degrees of freedom for the C^1 smooth space if the polynomial degree is high enough (4 if some additional conditions are fulfilled, 5 otherwise).

Our work further develops the underlying theory in the direction of [20, 8]. We set up our notation and framework in Sections 1 and 2. In Section 3 we define the class of analysis-suitable (AS) G^1 geometry parametrizations, which includes the bilinear ones and the extensions of [20, Section 3.4]. Then, in Section 5.1, we analyze the structure of C^1 isogeometric spaces over AS G^1 two-patch geometries. From that we can conclude the optimal order of approximation for p -degree isogeometric functions having C^1 continuity across the patch interface and up to C^{p-2}

continuity in the interface direction, and infer the C^1 locking for C^{p-1} continuity. On the other hand, in Section 5.2 we analyze C^1 isogeometric spaces constructed over more general geometries and conclude that h -convergence is suboptimal beyond AS G^1 geometries. The extensions to surface domains and to NURBS are briefly discussed in Sections 6 and 7, respectively. Numerical tests on two- and multi-patch domains are reported in Section 8. A key question that remains to be studied is the flexibility of AS G^1 parametrizations, as well as construction methods for AS G^1 parametrizations on general geometries. We hope this article offers an innovative point of view which leads to a better understanding of this difficult question. We summarize our experience and give conclusions in Section 9.

2. Planar multi-patch spline parametrizations and isogeometric spaces

Given an interval or a rectangle ω , we denote by $\mathcal{S}_r^p(\omega)$ the spline space of degree p (in each direction) and continuity C^r at all interior knots. The knot mesh in the parametric domain is assumed to be uniform, with mesh-size h (which is not explicitly indicated in the notation) and interior knot multiplicity $p-r$. We write \mathcal{S}_r^p instead of $\mathcal{S}_r^p(\omega)$ when the domain ω is obvious from the context. We allow $r \geq p$, which stands for C^∞ continuity, that is, the case of global tensor-product polynomials on ω . In this case we also use the notation $\mathcal{P}^p(\omega) = \mathcal{S}_p^p(\omega) = \mathcal{S}_{p+1}^p(\omega) = \dots$

Consider a planar multi-patch domain of interest

$$\Omega = \Omega^{(1)} \cup \dots \cup \Omega^{(N)} \subset \mathbb{R}^2, \quad (1)$$

where the closed sets $\Omega^{(i)}$ form a regular partition (with disjoint interior). For simplicity, we do not allow hanging nodes. Each $\Omega^{(i)}$ is assumed to be a spline patch, that is

$$\mathbf{F}^{(i)} : [0, 1] \times [0, 1] = \widehat{\Omega} \rightarrow \Omega^{(i)}, \quad (2)$$

where $\mathbf{F}^{(i)} \in \mathcal{S}_r^p(\widehat{\Omega}) \times \mathcal{S}_r^p(\widehat{\Omega})$. We assume

$$r \geq 1 \quad (3)$$

($r \geq p$ means we have Bezier patches $\Omega^{(i)}$) and we assume the parametrizations are not singular, i.e., for all i and for all $(u, v) \in \widehat{\Omega}$,

$$\det \begin{bmatrix} D_u \mathbf{F}^{(i)}(u, v) & D_v \mathbf{F}^{(i)}(u, v) \end{bmatrix} \neq 0. \quad (4)$$

For the sake of simplicity we do not consider more general configurations, e.g., non-uniform knot meshes, different degree or continuity parameters in each parametric direction, different continuity at different knots, or different spline spaces for different patches. Indeed, our simple configuration already presents the key features and difficulties we are interested in.

We assume global continuity of the patch parametrizations. This means the following. Let us fix $\Gamma = \Gamma^{(i,j)} = \Omega^{(i)} \cap \Omega^{(j)}$. When using the superscript as (i, j) in the paper, we assume implicitly that i and j are such that $\Gamma^{(i,j)}$ is not a point or an empty set. Let $\mathbf{F}^{(L)}, \mathbf{F}^{(R)}$ be given such that

$$\begin{aligned} \mathbf{F}^{(L)} &: [-1, 0] \times [0, 1] = \widehat{\Omega}^{(L)} \rightarrow \Omega^{(L)} = \Omega^{(i)}, \\ \mathbf{F}^{(R)} &: [0, 1] \times [0, 1] = \widehat{\Omega}^{(R)} \rightarrow \Omega^{(R)} = \Omega^{(j)}, \end{aligned} \quad (5)$$

where $(\mathbf{F}^{(L)})^{-1} \circ \mathbf{F}^{(i)}$ and $(\mathbf{F}^{(R)})^{-1} \circ \mathbf{F}^{(j)}$ are linear transformations (combinations of a translation, rotation and symmetry). Moreover, the parametrizations agree at $u = 0$, i.e., there is a $\mathbf{F}_0 : [0, 1] \rightarrow \mathbb{R}^2$ with

$$\Gamma = \{\mathbf{F}_0(v) = \mathbf{F}^{(L)}(0, v) = \mathbf{F}^{(R)}(0, v), v \in [0, 1]\}. \quad (6)$$

An example is depicted in Figure 2.

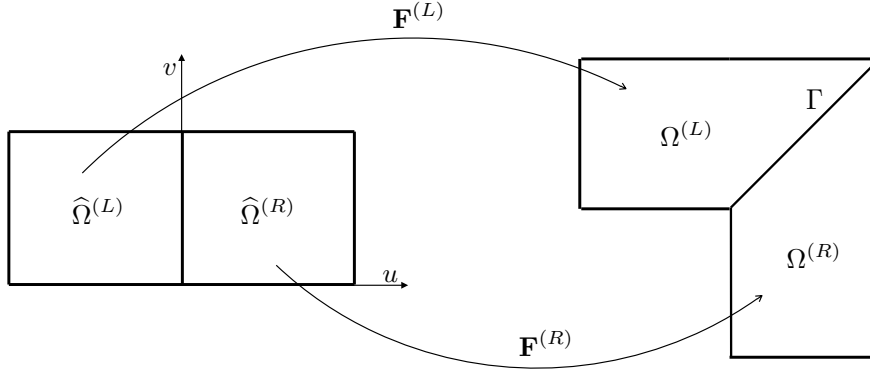


Figure 2: Example of the general setting of (5)–(6).

Remark 1. The domain $\Omega = \Omega^{(1)} \cup \dots \cup \Omega^{(N)}$ can be endowed with a spline manifold structure as defined in [28]. Each pair of adjacent subsets $\Omega^{(i)}$, $\Omega^{(j)}$ is naturally associated with a chart $[-1, 1] \times [0, 1] = \hat{\Omega}^{(L)} \cup \hat{\Omega}^{(R)}$ through the maps $\mathbf{F}^{(L)}$ and $\mathbf{F}^{(R)}$.

Definition 1 (Isogeometric spaces). The isogeometric space corresponding to \mathcal{S}_r^p and Ω is given as

$$\mathcal{V} = \left\{ \phi : \Omega \rightarrow \mathbb{R} \text{ such that } \phi \circ \mathbf{F}^{(i)} \in \mathcal{S}_r^p(\hat{\Omega}), i = 1, \dots, N \right\}. \quad (7)$$

Furthermore we have

$$\mathcal{V}^0 = \mathcal{V} \cap C^0(\Omega), \quad (8)$$

and

$$\mathcal{V}^1 = \mathcal{V} \cap C^1(\Omega). \quad (9)$$

The graph $\Sigma \subset \Omega \times \mathbb{R}$ of an isogeometric function $\phi : \Omega \rightarrow \mathbb{R}$ is naturally split into patches Σ^i having the parametrizations

$$\begin{bmatrix} \mathbf{F}^{(i)} \\ g^{(i)} \end{bmatrix} : [0, 1] \times [0, 1] = \hat{\Omega} \rightarrow \Sigma^i \quad (10)$$

where $g^{(i)} = \phi \circ \mathbf{F}^{(i)}$.

In order to analyze the smoothness of an isogeometric function along one interface $\Gamma = \Gamma^{(i,j)} = \Omega^{(i)} \cap \Omega^{(j)}$, we introduce

$$\begin{aligned} \begin{bmatrix} \mathbf{F}^{(L)} \\ g^{(L)} \end{bmatrix} &: [-1, 0] \times [0, 1] = \widehat{\Omega}^{(L)} \rightarrow \Sigma^{(i)} = \Sigma^{(L)}, \\ \begin{bmatrix} \mathbf{F}^{(R)} \\ g^{(R)} \end{bmatrix} &: [0, 1] \times [0, 1] = \widehat{\Omega}^{(R)} \rightarrow \Sigma^{(j)} = \Sigma^{(R)}, \end{aligned} \quad (11)$$

where $g^{(L)}, g^{(R)}$ are defined obviously as extensions of (5), see Figure 3. Continuity of ϕ is implied by the continuity of the graph parametrization, which we assume and set to

$$g_0(v) = g^{(L)}(0, v) = g^{(R)}(0, v), \quad (12)$$

for all $v \in [0, 1]$, analogous to (6).

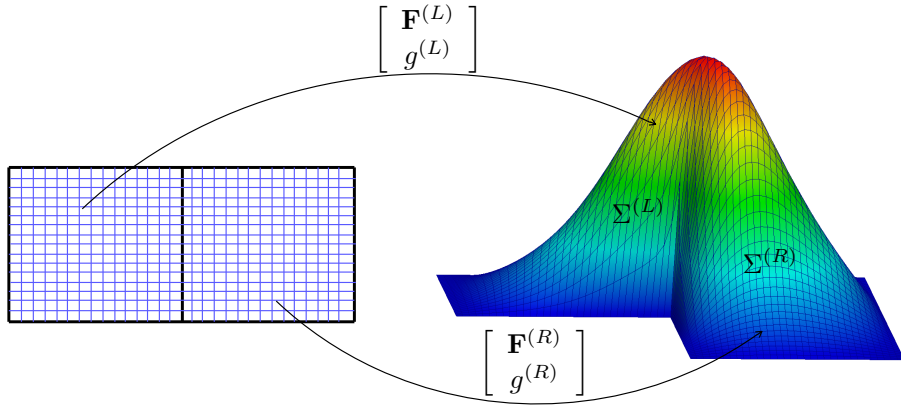


Figure 3: Example of the general setting of (11).

3. C^1 isogeometric spaces

If an isogeometric function is C^1 within each patch (condition (3)), with non-singular parametrization (condition (4)) and is globally continuous (condition (12)), then it is globally C^1 if and only if there exists a well defined tangent plane at each point of the interfaces $\Sigma^{(i)} \cap \Sigma^{(j)}$. Focusing on one interface, with notation (11), the tangent planes from the left and right sides are formed by the two pairs of vectors

$$\begin{bmatrix} D_u \mathbf{F}^{(L)}(0, v) \\ D_u g^{(L)}(0, v) \end{bmatrix} \text{ and } \begin{bmatrix} D_v \mathbf{F}_0(v) \\ D_v g_0(v) \end{bmatrix} \text{ as well as } \begin{bmatrix} D_u \mathbf{F}^{(R)}(0, v) \\ D_u g^{(R)}(0, v) \end{bmatrix} \text{ and } \begin{bmatrix} D_v \mathbf{F}_0(v) \\ D_v g_0(v) \end{bmatrix},$$

respectively. These are three different vectors (the vector tangent to $\Sigma^{(i)} \cap \Sigma^{(j)}$ is in common) that form a unique tangent plane, i.e. they are coplanar, if and only if they are linearly dependent. In

other words the isogeometric function ϕ is C^1 on $\Omega^{(i)} \cup \Omega^{(j)}$ if and only if

$$\det \begin{bmatrix} D_u \mathbf{F}^{(L)}(0, v) & D_u \mathbf{F}^{(R)}(0, v) & D_v \mathbf{F}_0(v) \\ D_u g^{(L)}(0, v) & D_u g^{(R)}(0, v) & D_v g_0(v) \end{bmatrix} = 0 \quad (13)$$

for all $v \in [0, 1]$. In the context of isogeometric methods, the domain Ω and its parametrization are given at the first stage, then (13) is the condition on the isogeometric function in parametric coordinates (i.e., $g^{(L)}$ and $g^{(R)}$) that gives C^1 continuity of the isogeometric function in physical coordinates.

In CAGD literature, condition (13) is named *geometric continuity of order 1*, in short G^1 , and is commonly stated as in the following Definition (see, e.g., [27, 23, 2]).

Definition 2 (G^1 -continuity at $\Sigma^{(i)} \cap \Sigma^{(j)}$). Given the parametrizations $\mathbf{F}^{(L)}$, $\mathbf{F}^{(R)}$, $g^{(L)}$, $g^{(R)}$ as in (5), (11), fulfilling (3), (4) and (12), we say that the graph parametrization is G^1 at the interface $\Sigma^{(i)} \cap \Sigma^{(j)}$ if there exist $\alpha^{(L)} : [0, 1] \rightarrow \mathbb{R}$, $\alpha^{(R)} : [0, 1] \rightarrow \mathbb{R}$ and $\beta : [0, 1] \rightarrow \mathbb{R}$ such that for all $v \in [0, 1]$,

$$\alpha^{(L)}(v)\alpha^{(R)}(v) > 0 \quad (14)$$

and

$$\alpha^{(R)}(v) \begin{bmatrix} D_u \mathbf{F}^{(L)}(0, v) \\ D_u g^{(L)}(0, v) \end{bmatrix} - \alpha^{(L)}(v) \begin{bmatrix} D_u \mathbf{F}^{(R)}(0, v) \\ D_u g^{(R)}(0, v) \end{bmatrix} + \beta(v) \begin{bmatrix} D_v \mathbf{F}_0(v) \\ D_v g_0(v) \end{bmatrix} = \mathbf{0}. \quad (15)$$

The sign condition (14) on $\alpha^{(L)}$ and $\alpha^{(R)}$ forbids, on general surfaces, the presence of cusps. However, for the graph of a function it is obvious.

For our study it is useful to express G^1 continuity as in Definition 2 since the coefficients $\alpha^{(L)}$, $\alpha^{(R)}$ and β play an important role. They are uniquely determined, up to a common multiplicative factor, by $\mathbf{F}^{(L)}$ and $\mathbf{F}^{(R)}$, i.e. from the equation

$$\alpha^{(R)}(v)D_u \mathbf{F}^{(L)}(0, v) - \alpha^{(L)}(v)D_u \mathbf{F}^{(R)}(0, v) + \beta(v)D_v \mathbf{F}_0(v) = \mathbf{0}. \quad (16)$$

Precisely, we have the following proposition which extends [8, Theorem 3].

Proposition 1. Consider $\mathbf{F}^{(L)}$, $\mathbf{F}^{(R)}$, $g^{(L)}$, $g^{(R)}$ fulfilling Definition 2. Then (15) holds if and only if $\alpha^{(S)}(v) = \gamma(v)\bar{\alpha}^{(S)}(v)$, for $S \in \{L, R\}$, and $\beta(v) = \gamma(v)\bar{\beta}(v)$, where

$$\bar{\alpha}^{(S)}(v) = \det \begin{bmatrix} D_u \mathbf{F}^{(S)}(0, v) & D_v \mathbf{F}_0(v)(0, v) \end{bmatrix}, \quad (17)$$

$$\bar{\beta}(v) = \det \begin{bmatrix} D_u \mathbf{F}^{(L)}(0, v) & D_u \mathbf{F}^{(R)}(0, v) \end{bmatrix}, \quad (18)$$

and $\gamma : [0, 1] \rightarrow \mathbb{R}$ is any function, with $\gamma(v) \neq 0$ if and only if (14) holds. Moreover

$$\beta(v) = \alpha^{(L)}(v)\beta^{(R)}(v) - \alpha^{(R)}(v)\beta^{(L)}(v), \quad (19)$$

where

$$\beta^{(S)}(v) = \frac{D_u \mathbf{F}^{(S)}(0, v) \cdot D_v \mathbf{F}_0(v)}{\|D_v \mathbf{F}_0(v)\|^2}, \quad S \in \{L, R\}. \quad (20)$$

Proof. Obviously (15) determines $\alpha^{(L)}(v)$, $\alpha^{(R)}(v)$ and $\beta(v)$ up to a common factor $\gamma(v)$ and, since the two vectors $D_u\mathbf{F}^{(L)}(0, v)$ and $D_v\mathbf{F}_0(v)$ are linearly independent because of (4), $\alpha^{(L)}(v)$, $\alpha^{(R)}(v)$ and $\beta(v)$ are uniquely determined up to a common factor $\gamma(v)$ by (16). We have

$$\det \begin{bmatrix} D_u\mathbf{F}^{(L)}(0, v) & D_u\mathbf{F}^{(R)}(0, v) & D_v\mathbf{F}_0(v)(0, v) \\ D_u\mathbf{F}^{(L)}(0, v) \cdot \mathbf{e}_k & D_u\mathbf{F}^{(R)}(0, v) \cdot \mathbf{e}_k & D_v\mathbf{F}_0(v)(0, v) \cdot \mathbf{e}_k \end{bmatrix} = 0, \quad (21)$$

for all $k = 1, 2$, \mathbf{e}_k being the canonical base vectors in \mathbb{R}^2 . Using the Laplace expansion of the above determinant (along the third row) we end up with

$$\bar{\alpha}^{(R)}(v)D_u\mathbf{F}^{(L)}(0, v) - \bar{\alpha}^{(L)}(v)D_u\mathbf{F}^{(R)}(0, v) + \bar{\beta}(v)D_v\mathbf{F}_0(v) = 0,$$

where $\bar{\alpha}^{(L)}$ and $\bar{\alpha}^{(R)}$ and $\bar{\beta}$ are as in (17) and (18). In a similar way (13) yields

$$\bar{\alpha}^{(R)}(v)D_u g^{(L)}(0, v) - \bar{\alpha}^{(L)}(v)D_u g^{(R)}(0, v) + \bar{\beta}(v)D_v g_0(v) = 0.$$

Setting

$$\boldsymbol{\nu}(v) = \begin{bmatrix} D_v\mathbf{F}_0(v) \cdot \mathbf{e}_2 \\ -D_v\mathbf{F}_0(v) \cdot \mathbf{e}_1 \end{bmatrix}, \quad \boldsymbol{\tau}(v) = \frac{D_v\mathbf{F}_0(v)}{\|D_v\mathbf{F}_0(v)\|^2},$$

we have

$$\det \begin{bmatrix} \boldsymbol{\nu}(v) & \boldsymbol{\tau}(v) \end{bmatrix} = 1 \quad \text{and} \quad \boldsymbol{\nu}(v) \cdot \boldsymbol{\tau}(v) = 0.$$

Using the expansion

$$\forall \mathbf{v} \in \mathbb{R}^2, \quad \mathbf{v} = \det \begin{bmatrix} \mathbf{v} & \boldsymbol{\tau}(v) \end{bmatrix} \boldsymbol{\nu}(v) - \det \begin{bmatrix} \mathbf{v} & \boldsymbol{\nu}(v) \end{bmatrix} \boldsymbol{\tau}(v),$$

then

$$\det \begin{bmatrix} \mathbf{v}^{(L)} & \mathbf{v}^{(R)} \end{bmatrix} = \det \begin{bmatrix} \mathbf{v}^{(L)} & \boldsymbol{\nu}(v) \end{bmatrix} \det \begin{bmatrix} \mathbf{v}^{(R)} & \boldsymbol{\tau}(v) \end{bmatrix} - \det \begin{bmatrix} \mathbf{v}^{(L)} & \boldsymbol{\tau}(v) \end{bmatrix} \det \begin{bmatrix} \mathbf{v}^{(R)} & \boldsymbol{\nu}(v) \end{bmatrix},$$

which gives (19) by choosing $\mathbf{v}^{(S)} = D_u\mathbf{F}^{(S)}(0, v)$, for $S \in \{L, R\}$. \square

Remark 2. If (15) holds, then there exist coefficients $\alpha^{(S)} \in \mathcal{S}_{r-1}^{2p-1}([0, 1])$, for $S \in \{L, R\}$, and $\beta \in \mathcal{S}_r^{2p}([0, 1])$. Indeed, this follows from Proposition 1 selecting $\gamma = 1$.

We remark that, in the context of isogeometric methods, we consider Ω and its parametrization given. Then $\alpha^{(L)}$, $\alpha^{(R)}$ and β are determined and C^1 continuity of isogeometric functions is equivalent to the last equation in (15), that is

$$\alpha^{(R)}(v)D_u g^{(L)}(0, v) - \alpha^{(L)}(v)D_u g^{(R)}(0, v) + \beta(v)D_v g_0(v) = 0 \quad (22)$$

for all $v \in [0, 1]$. In the next sections, we will indeed study the C^1 constraint in dependence of $\alpha^{(L)}$, $\alpha^{(R)}$ and β , by using (22).

We close this section with stating the equivalence between C^1 continuity of the isogeometric function and G^1 continuity of its graph parametrization as presented in [20] (see also [16] for a generalization to arbitrary dimension and continuity). We give a detailed proof here, based on the results of Proposition 1, which serves as a starting point for our further studies.

Proposition 2. *Consider the setting of Section 2. Then an isogeometric function $\phi \in \mathcal{V}$ belongs to \mathcal{V}^1 if and only if its graph Σ is G^1 continuous on each interface $\Sigma^{(i)} \cap \Sigma^{(j)}$.*

Proof. Consider a graph interface $\Sigma^{(i)} \cap \Sigma^{(j)}$ and the corresponding $\Gamma = \Gamma^{(i,j)} = \Omega^{(i)} \cap \Omega^{(j)}$. Define \mathbf{n} such that

$$\mathbf{n} \circ \mathbf{F}_0(v) = \frac{1}{\gamma(v) \|D_v \mathbf{F}_0(v)\|^2} \begin{bmatrix} D_v \mathbf{F}_0(v) \cdot \mathbf{e}_2 \\ -D_v \mathbf{F}_0(v) \cdot \mathbf{e}_1 \end{bmatrix}.$$

The vector \mathbf{n} is orthogonal to Γ , it is not in general unitary and it is continuous, since \mathbf{F}_0 is at least C^1 from (3).

For $S \in \{L, R\}$, let $\phi = g^{(S)} \circ [F^{(S)}]^{-1}$ on $\Omega^{(S)}$, then the normal derivative from side S fulfills

$$\nabla^{(S)} \phi(x, y) \cdot \mathbf{n}(x, y) = [D_u g^{(S)}(0, v) D_v g_0(v)] \left[D_u \mathbf{F}^{(S)}(0, v) D_v \mathbf{F}_0(v) \right]^{-1} \cdot \mathbf{n} \circ \mathbf{F}_0(v), \quad (23)$$

for all $(x, y) \in \Gamma$, where here and in what follows we implicitly assume the relation $\mathbf{F}_0(v) = (x, y)$. Using Cramer's rule as well as (17)–(20) we get

$$\begin{aligned} & \left[D_u \mathbf{F}^{(S)}(0, v) D_v \mathbf{F}_0(v) \right]^{-1} \cdot \mathbf{n} \circ \mathbf{F}_0(v) \\ &= \frac{\begin{bmatrix} D_v \mathbf{F}_0(v) \cdot \mathbf{e}_2 & -D_v \mathbf{F}_0(v) \cdot \mathbf{e}_1 \\ -D_u \mathbf{F}^{(S)}(0, v) \cdot \mathbf{e}_2 & D_u \mathbf{F}^{(S)}(0, v) \cdot \mathbf{e}_1 \end{bmatrix}}{\det \begin{bmatrix} D_u \mathbf{F}^{(S)}(0, v) & D_v \mathbf{F}_0(v) \end{bmatrix}} \cdot \mathbf{n} \circ \mathbf{F}_0(v) \\ &= \frac{\begin{bmatrix} 1 \\ -\beta^{(S)}(v) \end{bmatrix}}{\alpha^{(S)}(v)}. \end{aligned} \quad (24)$$

Substituting (24) back to (23) we then obtain

$$\nabla^{(S)} \phi(x, y) \cdot \mathbf{n}(x, y) = \frac{D_u g^{(S)}(0, v) - \beta^{(S)}(v) D_v g_0(v)}{\alpha^{(S)}(v)} \quad (25)$$

for $S \in \{R, L\}$. Therefore ϕ is C^1 continuous at $(x, y) \in \Gamma$, i.e.,

$$\nabla^{(L)} \phi(x, y) \cdot \mathbf{n}(x, y) = \nabla^{(R)} \phi(x, y) \cdot \mathbf{n}(x, y)$$

holds, if and only if (by (25))

$$\frac{D_u g^{(L)}(0, v) - \beta^{(L)}(v) D_v g_0(v)}{\alpha^{(L)}(v)} = \frac{D_u g^{(R)}(0, v) - \beta^{(R)}(v) D_v g_0(v)}{\alpha^{(R)}(v)}.$$

That, after multiplying both sides by $\alpha^{(L)}(v) \alpha^{(R)}(v)$ and using (19)–(20), is equivalent to (22). \square

Remark 3. *As a consequence of Proposition 2, C^1 isogeometric spaces over C^0 planar multi-patch parametrizations fit in the isoparametric framework.*

4. Analysis-suitable G^1 parametrizations

At each interface $\Gamma = \Gamma^{(i,j)} = \Omega^{(i)} \cap \Omega^{(j)}$, given any regular and orientation preserving $\mathbf{F}^{(L)}$, $\mathbf{F}^{(R)}$, as in (5), there exist coefficients $\alpha^{(L)}$, $\alpha^{(R)}$ and β , with $\alpha^{(L)}(v)\alpha^{(R)}(v) > 0$, such that (16) holds. The coefficients are given by Proposition 1. However, optimal convergence properties of the isogeometric space on Ω require conditions on the geometry parametrization that can be stated as restrictions on $\alpha^{(L)}$, $\alpha^{(R)}$ and β , as in the definition below.

Definition 3 (Analysis-suitable G^1 -continuity). $\mathbf{F}^{(L)}$ and $\mathbf{F}^{(R)}$ are *analysis-suitable G^1 -continuous* at the interface Γ (in short, AS $G^1(\Gamma)$ or AS G^1) if there exist $\alpha^{(L)}, \alpha^{(R)}, \beta^{(L)}, \beta^{(R)} \in \mathcal{P}^1([0, 1])$ such that (16) and (19) hold, that is for all $v \in [0, 1]$

$$\alpha^{(R)}(v)D_u\mathbf{F}^{(L)}(0, v) - \alpha^{(L)}(v)D_u\mathbf{F}^{(R)}(0, v) = (\alpha^{(R)}(v)\beta^{(L)}(v) - \alpha^{(L)}(v)\beta^{(R)}(v))D_v\mathbf{F}_0(v).$$

Remark 4. As in Remark 3, we observe that C^1 isogeometric spaces over AS G^1 multi-patch parametrizations fit in the isoparametric framework.

The class of AS G^1 parametrizations contains the bilinear ones.

Proposition 3. Any $\mathbf{F}^{(L)} \in \mathcal{P}^1(\Omega^{(L)}) \times \mathcal{P}^1(\Omega^{(L)})$ and $\mathbf{F}^{(R)} \in \mathcal{P}^1(\Omega^{(R)}) \times \mathcal{P}^1(\Omega^{(R)})$ are AS G^1 -continuous at Γ . Moreover, for any $\alpha^{(L)}, \alpha^{(R)} \in \mathcal{P}^1([0, 1])$ strictly positive and $\beta^{(L)}, \beta^{(R)} \in \mathcal{P}^1([0, 1])$ there exist $\mathbf{F}^{(L)} \in \mathcal{P}^1(\Omega^{(L)})$ and $\mathbf{F}^{(R)} \in \mathcal{P}^1(\Omega^{(R)})$ fulfilling (16).

Proof. The statement follows directly from Proposition 1. □

Remark 5. The class of AS G^1 parametrizations is wider than only bilinear. We will show some examples later in Section 8 (see also [20, Section 3.4]). If $\mathbf{F}^{(L)}$ and $\mathbf{F}^{(R)}$ are analysis-suitable G^1 -continuous at Γ but not bilinear, and $\alpha^{(L)}$, $\alpha^{(R)}$, $\beta^{(L)}$ and $\beta^{(R)}$ are as in Definition 3, then $\gamma \neq 1$ in Proposition 1. In any case $\gamma \in C^{r-1}([0, 1])$.

5. Two-patch geometry

In this section we analyze the two-patch geometry. This is the simplest geometric configuration allows us to focus on the C^1 -continuity constraints that are associated with each patch interface, which is also a key step in more general configurations.

For the space of isogeometric C^0 functions, that is \mathcal{V}^0 defined in (7)-(8), optimal convergence under h -refinement is known since the results in [1, 6] applies directly. C^1 -continuity further constrains traces and (normal) derivatives at Γ of functions $\phi \in \mathcal{V}^1$ (from (9)). Therefore the approximation properties of the space \mathcal{V}^1 follow from the ones of traces of functions and normal derivatives of functions of \mathcal{V}^1 at Γ . Thus we introduce the space of traces and normal derivatives on Γ

$$\mathcal{V}_\Gamma^1 = \{ \Gamma \ni (x, y) \mapsto [\phi(x, y), \nabla\phi(x, y) \cdot \mathbf{n}(x, y)], \text{ such that } \phi \in \mathcal{V}^1 \} \quad (26)$$

and its pullback

$$\widehat{\mathcal{V}}_\Gamma^1 = \{ [\phi, \nabla\phi \cdot \mathbf{n}] \circ \mathbf{F}_0, \text{ such that } \phi \in \mathcal{V}^1 \} \quad (27)$$

where, for all $v \in [0, 1]$,

$$\mathbf{n} \circ \mathbf{F}_0(v) = \frac{1}{\gamma(v) \|D_v \mathbf{F}_0(v)\|^2} \begin{bmatrix} D_v \mathbf{F}_0(v) \cdot \mathbf{e}_2 \\ -D_v \mathbf{F}_0(v) \cdot \mathbf{e}_1 \end{bmatrix}.$$

Observe that the normal \mathbf{n} defined above is not unitary in general and is in $C^{r-1}([0, 1])$ as a function of v (see Remark 5). With this choice we have that $[\phi, \nabla \phi \cdot \mathbf{n}] \circ \mathbf{F}_0 = [g_0, g_1]$ is equivalent to

$$g^{(S)}(u, v) = g_0(v) + (\beta^{(S)}(v)g'_0(v) + \alpha^{(S)}(v)g_1(v))u + O(u^2), \quad (28)$$

thanks to (25). Note that the trace in $\widehat{\mathcal{V}}_\Gamma^1$ fulfills $\phi \circ \mathbf{F}_0 \in \mathcal{S}_r^p$. This is not true for the normal derivative, which in general is a NURBS function of some degree higher than p , see [33].

5.1. AS G^1 -continuous two-patch geometry

The next result gives the key properties of the space $\widehat{\mathcal{V}}_\Gamma^1$ (defined in (27)) in the case of AS G^1 parametrizations.

Theorem 1. *Let $\Omega = \Omega^{(L)} \cup \Omega^{(R)}$, and let $\mathbf{F}^{(L)}$ and $\mathbf{F}^{(R)}$ be AS G^1 at the interface $\Gamma = \partial\Omega^{(L)} \cup \partial\Omega^{(R)}$. Then*

$$\mathcal{S}_{r+1}^p([0, 1]) \times \mathcal{S}_r^{p-1}([0, 1]) \subset \widehat{\mathcal{V}}_\Gamma^1. \quad (29)$$

Proof. For linear $\alpha^{(S)}$ and $\beta^{(S)}$ ($S \in \{L, R\}$) and $[g_0, g_1] \in \mathcal{S}_{r+1}^p([0, 1]) \times \mathcal{S}_r^{p-1}([0, 1])$, we have

$$g^{(S)}(u, v) = g_0(v) + (\beta^{(S)}(v)g'_0(v) + \alpha^{(S)}(v)g_1(v))u \in \mathcal{S}_r^p(\widehat{\Omega}^{(S)}). \quad (30)$$

Then the statement is a direct consequence of (28). \square

Theorem 1 guarantees that the trace space for the function value $\{\phi \circ \mathbf{F}_0 : \phi \in \mathcal{V}^1\}$ includes all splines of degree p and regularity at least $r + 1$, and independently the trace space for the normal derivatives of the function $\{(\nabla \phi \cdot \mathbf{n}) \circ \mathbf{F}_0 : \phi \in \mathcal{V}^1\}$ includes all splines of degree $p - 1$ and regularity at least r . From this one can conclude the optimal order of approximation of \mathcal{V}_Γ^1 and consequently of the whole space \mathcal{V}^1 when $r < p - 1$.

However, if $r = p - 1$ and the parametrization is not trivial, the space \mathcal{V}_Γ^1 suffers of C^1 locking, that is, h -refinement does not improve the approximation properties for ϕ and $\nabla \phi \cdot \mathbf{n}$ independently. This is stated in the next theorem.

Theorem 2. *Let $\Omega = \Omega^{(L)} \cup \Omega^{(R)}$, $\mathbf{F}^{(L)}$, $\mathbf{F}^{(R)}$ be AS G^1 at the interface $\Gamma = \Omega^{(L)} \cap \Omega^{(R)}$, and $r = p - 1$. Furthermore, let \mathcal{G}_0 and \mathcal{G}_1 be two spaces such that*

$$\mathcal{G}_0 \times \mathcal{G}_1 \subseteq \widehat{\mathcal{V}}_\Gamma^1. \quad (31)$$

If either $\beta^{(L)} \neq 0$ or $\beta^{(R)} \neq 0$ then the dimension of \mathcal{G}_0 is independent of h . If $\alpha^{(L)}$ and $\alpha^{(R)}$ are linearly independent, then the dimension of \mathcal{G}_1 is independent of h .

Proof. Let $[g_0, 0] = [\phi, \nabla\phi \cdot \mathbf{n}] \circ \mathbf{F}_0$ and assume that $\beta^{(L)}$ is a linear function not identically zero. Furthermore assume that if there exists a $v_0 \in [0, 1]$, such that $\beta^{(L)}(v_0) = 0$, then $\beta^{(R)}(v_0) \neq 0$. Using (28), i.e.,

$$g^{(S)}(u, v) = g_0(v) + \beta^{(S)}(v)g'_0(v)u + O(u^2),$$

and using $g^{(S)}(u, v) \in \mathcal{S}_{p-1}^p(\hat{\Omega}^{(S)})$ then first g_0 is a spline in $\mathcal{S}_{p-1}^p([0, 1])$ and second g'_0 is C^{p-1} , therefore g_0 is in fact a degree p global polynomial. The same conclusion holds when there exists a $v_0 \in [0, 1]$ such that $\beta^{(L)}(v_0) = \beta^{(R)}(v_0) = 0$ but v_0 is not a knot of the spline space $\mathcal{S}_{p-1}^p([0, 1])$ under consideration. If, instead, $\beta^{(L)}(v_0) = \beta^{(R)}(v_0) = 0$ and v_0 is a knot of the spline space $\mathcal{S}_{p-1}^p([0, 1])$, then g_0 has in general $p - 1$ continuous derivatives at v_0 . In conclusion if $g_0 \in \mathcal{G}_0$ then it has to be piecewise polynomial of degree p on at most two intervals, and is in $C^{p-1}([0, 1])$ globally. Hence the dimension of \mathcal{G}_0 is at most $p + 2$.

Take now $[0, g_1] = [\phi, \nabla\phi \cdot \mathbf{n}] \circ \mathbf{F}_0$ and assume $\alpha^{(L)}$ and $\alpha^{(R)}$ are linearly independent, that is, their linear combination gives the whole space $\mathcal{P}^p([0, 1])$. Now (28), i.e.,

$$g^{(S)}(u, v) = \alpha^{(S)}(v)g_1(v)u + O(u^2),$$

after taking the derivative in the variable u and evaluating at $u = 0$ gives

$$\frac{\partial}{\partial u}g^{(S)}(0, v) = \alpha^{(S)}(v)g_1(v),$$

and, by suitable linear combination for $S = L$ and $S = R$ yields

$$C_L \frac{\partial}{\partial u}g^{(L)}(0, v) + C_R \frac{\partial}{\partial u}g^{(R)}(0, v) = g_1(v).$$

Since $g^{(S)}(u, v) \in \mathcal{S}_{p-1}^p(\hat{\Omega}^{(S)})$, $g_1 \in \mathcal{S}_{p-1}^p([0, 1])$. Similarly

$$C'_L \frac{\partial}{\partial u}g^{(L)}(0, v) + C'_R \frac{\partial}{\partial u}g^{(R)}(0, v) = vg_1(v),$$

which means that $g_1 \in \mathcal{S}_{p-1}^{p-1}([0, 1])$, therefore the dimension of \mathcal{G}_1 is at most $p + 1$. \square

We need to explain the meaning and consequences of Theorem 2. If for all spaces \mathcal{G}_0 and \mathcal{G}_1 such that $\mathcal{G}_0 \times \mathcal{G}_1 \subseteq \widehat{\mathcal{V}}_\Gamma^1$ either the dimension of \mathcal{G}_0 or \mathcal{G}_1 is independent of the mesh size h then it means that we cannot gain approximation by h -refinement on both the traces and derivatives at Γ , that is, we are in the situation that we refer to as C^1 locking. This happens, according to Theorem 1, unless $\beta^{(L)} = \beta^{(R)} = 0$ and $\alpha^{(L)}$ and $\alpha^{(R)}$ are linearly dependent. However if $\beta^{(L)} = \beta^{(R)} = 0$ and for all $v \in [0, 1]$ we have $\alpha^{(L)}(v) = C\alpha^{(R)}(v)$ then

$$D_u \mathbf{F}^{(L)}(0, v) = CD_u \mathbf{F}^{(R)}(0, v).$$

That is, the parametrization is trivially G^1 in the sense that it can be made C^1 by scaling the variable u by a multiplicative factor in one of the two patches. If we are in such a case, as for C^1 parametrizations, one can easily conclude $\mathcal{S}_r^p([0, 1]) \times \mathcal{S}_r^p([0, 1]) = \widehat{\mathcal{V}}_\Gamma^1$.

We summarize in the following property the expected approximation properties of the isogeometric space \mathcal{V}^1 over AS G^1 parametrizations.

Corollary 1. *Optimal order of convergence for h -refinement can be achieved if $\mathbf{F}^{(L)}$ and $\mathbf{F}^{(R)}$ are AS G^1 and if $r \leq p - 2$. On the other hand, with the exclusion of geometry parametrizations that are C^1 up to a linear scaling in the variable u , splines of maximal smoothness $r = p - 1$ do not converge under h -refinement (C^1 locking).*

5.2. General two-patch geometry

In this section we study the approximation property of \mathcal{V}^1 , through the structure of the trace space $\widehat{\mathcal{V}}_\Gamma^1$ for two-patch geometry parametrizations beyond analysis-suitable G^1 -continuity. For this purpose, we consider the case where $\mathbf{F}^{(L)}$ is the identity mapping, which gives

$$\begin{aligned}\alpha^{(L)}(v) &= 1 \\ \alpha^{(R)}(v) &= D_u \mathbf{F}^{(R)}(0, v) \cdot \mathbf{e}_1 \in \mathcal{S}_r^p([0, 1]) \\ \beta^{(L)}(v) &= 0 \\ \beta^{(R)}(v) &= D_u \mathbf{F}^{(R)}(0, v) \cdot \mathbf{e}_2 \in \mathcal{S}_r^p([0, 1]),\end{aligned}\tag{32}$$

by selecting $\gamma(v) = 1$. Moreover $\mathbf{n} = \mathbf{e}_1$ and

$$\mathcal{V}_\Gamma^1 = \widehat{\mathcal{V}}_\Gamma^1 = \left\{ \left[\phi, \frac{\partial \phi}{\partial x} \right] \circ \mathbf{F}_0, \text{ such that } \phi \in \mathcal{V}^1 \right\}.\tag{33}$$

Equation (28) simplifies to

$$\begin{aligned}\left[\phi, \frac{\partial \phi}{\partial x} \right] \circ \mathbf{F}_0 &= [g_0, g_1] \\ \Leftrightarrow \begin{cases} g^{(L)}(u, v) = g_0(v) + g_1(v)u + O(u^2), \\ g^{(R)}(u, v) = g_0(v) + (\beta^{(R)}(v)g_0'(v) + \alpha^{(R)}(v)g_1(v))u + O(u^2). \end{cases}\end{aligned}\tag{34}$$

Comparing (34) to (28), we see that by suitably selecting $\mathbf{F}^{(R)}$, we obtain the whole set of relevant constraints on the parametrization $g^{(R)}$. The following statement gives a full characterization of the space $\widehat{\mathcal{V}}_\Gamma^1$. We use $\mathcal{S}_r^{-1}([0, 1])$ to indicate the null space \emptyset , and we recall that $p_\alpha = 0$ is not allowed.

Theorem 3. *Let $\Omega = \Omega^{(L)} \cup \Omega^{(R)}$, $\mathbf{F}^{(L)}$ be the identity and $\alpha^{(R)} \in \mathcal{S}_r^{p_\alpha}([0, 1])$, with $\alpha^{(R)} \notin \mathcal{S}_r^{p_\alpha - 1}([0, 1])$.*

If $\beta^{(R)} = 0$, then

$$\widehat{\mathcal{V}}_\Gamma^1 = \mathcal{S}_r^p([0, 1]) \times \mathcal{S}_r^{-p_\alpha}([0, 1]).\tag{35}$$

If instead $\beta^{(R)} \in \mathcal{S}_r^{p_\beta}([0, 1])$ with $\beta^{(R)} \notin \mathcal{S}_r^{p_\beta - 1}([0, 1])$, then

$$\widehat{\mathcal{V}}_\Gamma^1 = \mathcal{S}_{r+1}^{\min\{p, p - p_\beta + 1\}}([0, 1]) \times \mathcal{S}_r^{-p_\alpha}([0, 1]).\tag{36}$$

Proof. Since $\mathbf{F}^{(L)}$ is the identity we have $\widehat{\mathcal{V}}_\Gamma^1 \subset \mathcal{S}_r^p([0, 1]) \times \mathcal{S}_r^p([0, 1])$.

Consider first the case $\beta^{(R)} = 0$. It is easy to see that

$$\widehat{\mathcal{V}}_\Gamma^1 \supset \mathcal{S}_r^p([0, 1]) \times \mathcal{S}_r^{-p_\alpha}([0, 1]).$$

Indeed, given any $[g_0, g_1] \in \mathcal{S}_r^p([0, 1]) \times \mathcal{S}_r^{p-p_\alpha}([0, 1])$ we can find $g^{(S)}(u, v) \in \mathcal{S}_r^p(\hat{\Omega}^{(S)})$ such that (34) holds. In particular, take

$$g^{(R)}(u, v) = g_0(v) + \alpha^{(R)}(v)g_1(v)u.$$

Moreover, $\mathcal{S}_r^p([0, 1]) \times \mathcal{S}_r^{p-p_\alpha}([0, 1])$ is equal to the space $\widehat{\mathcal{V}}_\Gamma^1$ due to the second condition in (34), which is

$$g^{(R)}(u, v) = g_0(v) + \alpha^{(R)}(v)g_1(v)u + O(u^2)$$

for $\beta^{(R)} = 0$, since $g^{(R)}(u, v) \in \mathcal{S}_r^p(\hat{\Omega}^{(R)})$ forbids g_1 to be of a polynomial degree higher than $p - p_\alpha$.

The second case, $\beta^{(R)} \in \mathcal{S}_r^{p_\beta}([0, 1])$ with $\beta^{(R)} \notin \mathcal{S}_r^{p_\beta-1}([0, 1])$, is similar. Again, we have $\widehat{\mathcal{V}}_\Gamma^1 \supset \mathcal{S}_{r+1}^{\min\{p, p-p_\beta+1\}}([0, 1]) \times \mathcal{S}_r^{p-p_\alpha}([0, 1])$. Indeed, given any

$$[g_0, g_1] \in \mathcal{S}_{r+1}^{\min\{p, p-p_\beta+1\}}([0, 1]) \times \mathcal{S}_r^{p-p_\alpha}([0, 1])$$

we can find $g^{(S)}(u, v) \in \mathcal{S}_r^p(\hat{\Omega}^{(S)})$ such that (34) holds. This time, take

$$g^{(R)}(u, v) = g_0(v) + (\beta^{(R)}(v)g_0'(v) + \alpha^{(R)}(v)g_1(v))u.$$

As before $\mathcal{S}_{r+1}^{\min\{p, p-p_\beta+1\}}([0, 1]) \times \mathcal{S}_r^{p-p_\alpha}([0, 1])$ is equal to the space $\widehat{\mathcal{V}}_\Gamma^1$ due to the second condition in (34), that is

$$\mathcal{S}_r^p(\hat{\Omega}^{(R)}) \ni g^{(R)}(u, v) = g_0(v) + (\beta^{(R)}(v)g_0'(v) + \alpha^{(R)}(v)g_1(v))u + O(u^2).$$

This concludes the proof. □

Remark 6. In the setting of this section, $\mathbf{F}^{(L)}$ being the identity and $\mathbf{F}^{(R)} \in \mathcal{S}_r^p(\hat{\Omega}^{(R)}) \times \mathcal{S}_r^p(\hat{\Omega}^{(R)})$, we always have $p_\alpha \leq p$, $p_\beta \leq p$, which follows from (32). Then Theorem 3 guarantees

$$\mathcal{V}_\Gamma^1 = \widehat{\mathcal{V}}_\Gamma^1 \supset \mathcal{S}_p^1([0, 1]) \times \mathcal{S}_{p-1}^0([0, 1]) = \mathcal{P}^1 \times \mathcal{P}^0.$$

This is in accordance with the well known fact that isoparametric functions reproduce all linear polynomials.

Corollary 2. Optimal order of convergence for h -refinement can not be achieved if $\deg \alpha^{(R)} > 1$ or $\deg \beta^{(R)} > 1$. In particular, due to C^1 locking, there is no convergence for $\deg \alpha^{(R)} \geq p - r$ or $\deg \beta^{(R)} \geq p - r$.

Some examples will be considered and further analyzed in Section 8.

6. C^1 isogeometric spaces on surfaces

The result of the previous sections can be extended to three dimensions (and higher). In this section we consider domains in higher-dimension. The two relevant cases are volumes and surfaces. We discuss the latter, which is the most interesting in this context. We therefore consider a multi-patch surface

$$\Omega = \Omega^{(1)} \cup \dots \cup \Omega^{(N)} \subset \mathbb{R}^3.$$

We can set up an isogeometric function space over the surface

$$\mathcal{V} = \left\{ \phi : \Omega \rightarrow \mathbb{R} \text{ such that } \phi \circ \mathbf{F}^{(i)} \in \mathcal{S}_r^p(\widehat{\Omega}), i = 1, \dots, N \right\}, \quad (37)$$

and again $\mathcal{V}^0 = \mathcal{V} \cap C^0(\Omega)$ and $\mathcal{V}^1 = \mathcal{V} \cap C^1(\Omega)$. As for the planar case, $\mathbf{F}^{(i)} : \widehat{\Omega} \rightarrow \Omega^{(i)}$, though $\Omega^{(i)}$ is now a surface patch. More important, for the function space $C^1(\Omega)$ to be well defined, the surface Ω itself needs to be C^1 , i.e., the surface needs to have a well defined tangent plane in every point. For simplicity, we focus on a single interface, that is a two-patch geometry, where each patch is parameterized via

$$\begin{aligned} \mathbf{F}^{(L)} : [-1, 0] \times [0, 1] &= \widehat{\Omega}^{(L)} \rightarrow \Omega^{(L)} \subset \mathbb{R}^3, \\ \mathbf{F}^{(R)} : [0, 1] \times [0, 1] &= \widehat{\Omega}^{(R)} \rightarrow \Omega^{(R)} \subset \mathbb{R}^3 \end{aligned} \quad (38)$$

with $\mathbf{F}^{(S)} \in (\mathcal{S}_r^p(\widehat{\Omega}^{(S)}))^3$ for $S \in \{L, R\}$. We ask the parameterization to be G^1 , i.e., there exist $\alpha^{(L)} : [0, 1] \rightarrow \mathbb{R}$, $\alpha^{(R)} : [0, 1] \rightarrow \mathbb{R}$ and $\beta : [0, 1] \rightarrow \mathbb{R}$ such that $\forall v \in [0, 1]$, $\alpha^{(L)}(v)\alpha^{(R)}(v) > 0$ and

$$\alpha^{(R)}(v)D_u\mathbf{F}^{(L)}(0, v) - \alpha^{(L)}(v)D_u\mathbf{F}^{(R)}(0, v) + \beta(v)D_v\mathbf{F}_0(v) = \mathbf{0}. \quad (39)$$

Then, the surface gradient of a function $\phi : \Omega \rightarrow \mathbb{R}$ can be computed as follows. First, the surface Ω is extended to $\Omega_\epsilon \subset \mathbb{R}^3$ by defining

$$\mathbf{G}^{(S)} : \widehat{\Omega}^{(S)} \times]-\epsilon, \epsilon[\rightarrow \Omega_\epsilon^{(S)} \quad (40)$$

with

$$\mathbf{G}^{(S)}(u, v, w) = \mathbf{F}^{(S)}(u, v) + w\mathbf{N}^{(S)}(u, v), \quad (41)$$

where $\mathbf{N}^{(S)}$ is the unit normal vector of $\Omega^{(S)}$. Now, we define the extension Φ of the function ϕ via $\widehat{\Phi}^{(S)}(u, v, w) = \widehat{\phi}^{(S)}(u, v)$ for $S \in \{L, R\}$. The surface gradient of ϕ is then given as the three-dimensional gradient of the extension Φ in Ω_ϵ restricted to the surface Ω , i.e.

$$\nabla_\Omega \phi = \nabla \Phi|_\Omega, \quad (42)$$

where

$$\nabla \Phi \circ \mathbf{G}^{(S)} = \nabla \widehat{\Phi}^{(S)} \cdot (\nabla \mathbf{G}^{(S)})^{-1} \text{ on } \widehat{\Omega}^{(S)}. \quad (43)$$

By construction, the gradient is tangential to the surface.

Proposition 2 can be generalized to surface domains. For the sake of simplicity we consider a simplified case, by assuming that $\mathbf{F}^{(S)}$ can be projected onto the (x, y) -plane without self intersections. Then we have

$$\mathbf{F}^{(S)} = (F_1^{(S)}, F_2^{(S)}, F_3^{(S)})^T = (\mathbf{P}^{(S)}, f_3^{(S)} \circ \mathbf{P}^{(S)})^T \quad (44)$$

where $\mathbf{P}^{(S)} = (F_1^{(S)}, F_2^{(S)})^T$ is the planar parameterization of the projected surface and f_3 is an (isogeometric) function from the planar projection $\bar{\Omega}^{(S)} = \mathbf{P}^{(S)}(\widehat{\Omega}^{(S)})$ to \mathbb{R} . Then the following result is a direct corollary of Proposition 2.

Proposition 4. *An isogeometric function $\phi \in \mathcal{V}$ as in (37) belongs to \mathcal{V}^1 if and only if its graph Σ as a 2-dimensional surface in \mathbb{R}^4 is G^1 -continuous at each interface $\Sigma^{(i)} \cap \Sigma^{(j)}$.*

The definition for a G^1 -continuous graph of an isogeometric function ϕ is formally the same as in Definition 2, however now the graph of $\phi : \Omega \rightarrow \mathbb{R}$ is a two-dimensional surface in \mathbb{R}^4 . As for planar domains considered in Section 3, the coefficients for the G^1 condition are still determined by the parameterization $\mathbf{F}^{(S)}$, in fact by two of its three components. In our simplified case, we are in the following situation.

Proposition 5. *Consider surface patches*

$$\mathbf{F}^{(L)} = (\mathbf{P}^{(L)}, F_3^{(L)})^T, \quad \mathbf{F}^{(R)} = (\mathbf{P}^{(R)}, F_3^{(R)})^T$$

and functions $g^{(L)}, g^{(R)}$ fulfilling Definition 2. Then the coefficients $\alpha^{(L)}$ and $\alpha^{(R)}$ and β in (15) are given by $\alpha^{(S)}(v) = \gamma(v)\bar{\alpha}^{(S)}(v)$, for $S \in \{L, R\}$, and $\beta(v) = \gamma(v)\bar{\beta}(v)$, where

$$\bar{\alpha}^{(S)}(v) = \det \begin{bmatrix} D_u \mathbf{P}^{(S)}(0, v) & D_v \mathbf{P}^{(S)}(0, v) \end{bmatrix}, \quad (45)$$

$$\bar{\beta}(v) = \det \begin{bmatrix} D_u \mathbf{P}^{(L)}(0, v) & D_u \mathbf{P}^{(R)}(0, v) \end{bmatrix}, \quad (46)$$

and $\gamma : [0, 1] \rightarrow \mathbb{R}$ is any function with $\gamma(v) \neq 0$ if and only if $\alpha^{(L)}(v)\alpha^{(R)}(v) > 0$. Moreover

$$\beta(v) = \alpha^{(L)}(v)\beta^{(R)}(v) - \alpha^{(R)}(v)\beta^{(L)}(v), \quad (47)$$

where

$$\beta^{(S)}(v) = \frac{D_u \mathbf{P}^{(S)}(0, v) \cdot D_v \mathbf{P}^{(S)}(0, v)}{\|D_v \mathbf{P}^{(S)}(0, v)\|^2}, \quad S \in \{L, R\}. \quad (48)$$

Again, we omit the details of the proof, as it is a direct consequence of Proposition 1.

As for the planar case, optimal approximation properties of the isogeometric space hold when restricting the geometry parametrization to the class of analysis-suitable G^1 -continuous functions. The definition is omitted being exactly the same as Definition 3. In the case of (44), the parametrization $\mathbf{P}^{(S)}$ of the planar projection $\bar{\Omega}$ of the geometry Ω needs to be AS G^1 . Furthermore, the third component $F_3^{(S)}$ of $\mathbf{F}^{(S)}$ as well as the function $\hat{\phi}^{(S)}$ have to fulfill the same conditions, for $S \in \{L, R\}$. This means that Remarks 3–4 extend to surfaces: C^1 isogeometric spaces over G^1 and AS G^1 multi-patch parametrizations fit in the isoparametric framework. Eventually, $\phi \in \mathcal{V}^1(\Omega)$ if and only if $\bar{\phi} \in \mathcal{V}^1(\bar{\Omega})$, where $\bar{\phi} \circ \mathbf{P}^{(S)} = \phi \circ \mathbf{F}^{(S)}$. Then, the conclusions of Section 5 apply directly to AS G^1 surfaces, at least when the geometry parametrization fulfills (44). In fact, the same holds in general, but dealing with it is more technical and not reported for brevity.

Remark 7. *As a consequence of Proposition 5, C^1 isogeometric spaces over G^1 multi-patch surface parametrizations fit in the isoparametric framework.*

7. NURBS spaces

The results presented in Sections 3–5 are not limited to spline spaces, but, for example, are generalizable to NURBS. One possibility is to generate rational planar geometries from AS G^1 surface patches. A rational patch

$$\mathbf{F}^{(i)} : \hat{\Omega} \rightarrow \Omega^{(i)} \subset \mathbb{R}^2 \quad (49)$$

with

$$\mathbf{F}^{(i)} = \begin{pmatrix} F_1^{(i)} & F_2^{(i)} \\ F_3^{(i)} & F_3^{(i)} \end{pmatrix}^T \quad (50)$$

can be interpreted as a surface patch in \mathbb{R}^3 , with

$$\tilde{\mathbf{F}}^{(i)} = \left(F_1^{(i)}, F_2^{(i)}, F_3^{(i)} \right)^T, \quad (51)$$

when transformed to homogeneous coordinates. Recall, that two points $\tilde{\mathbf{F}}, \tilde{\mathbf{F}}'$ in homogeneous coordinates correspond to the same point in Euclidean space, if there exists a $\lambda \neq 0$ such that $\tilde{\mathbf{F}} = \lambda \tilde{\mathbf{F}}'$. An AS G^1 surface with surface patches (51) generates a rational AS G^1 geometry via (50). Therefore this construction fits into the framework of Section 6. For the sake of brevity, we only present one example (Figure 7) in the next Section 8.2.2 and postpone further studies. We want to point out that not all multi-patch NURBS geometries fit into this framework. The surface representation in (51) may not be G^1 (or not even C^0) but the rational patches representing the graph still join G^1 . Such a configuration is given for the circle presented in Figure 16. However, in that example the graph surface is not analysis-suitable G^1 .

8. Numerical tests

In this section, we present numerical tests which illustrate the previous theoretical results. The simulations have been obtained by the isogeometric analysis library IGATools, see [26] for an introduction.

8.1. Model problem

We consider the following bilaplacian problem on $\Omega \subset \mathbb{R}^2$, where the unknown is denoted by w and the data by f ,

$$\begin{cases} \Delta^2 w = f & \Omega, \\ w = 0 & \partial\Omega, \\ \nabla w \cdot \mathbf{n} = 0 & \partial\Omega. \end{cases} \quad (52)$$

In our tests the data f is selected in order to have an analytic exact solution w . Let

$$\mathcal{U}_0 = \{v \in H^2(\Omega), v = 0 \text{ on } \partial\Omega \text{ and } \nabla v \cdot \mathbf{n} = 0 \text{ on } \partial\Omega\},$$

the variational form of (52) is, find $w \in \mathcal{U}_0$, such that

$$\int_{\Omega} \Delta w \Delta v \, dx \, dy = \int_{\Omega} f v \, dx \, dy, \quad \forall v \in \mathcal{U}_0. \quad (53)$$

In what follows, we consider two types of geometries, the ones which are analysis-suitable G^1 and the ones which are not. Let us start with the analysis-suitable G^1 geometries.

8.2. Analysis-suitable G^1 geometries

We consider five different analysis-suitable G^1 geometry mappings with different numbers of patches. For all cases, we select the degrees $p = 3, 4, 5$ and regularities $1 \leq r \leq p - 1$.

8.2.1. Two-patch geometry (L-shape)

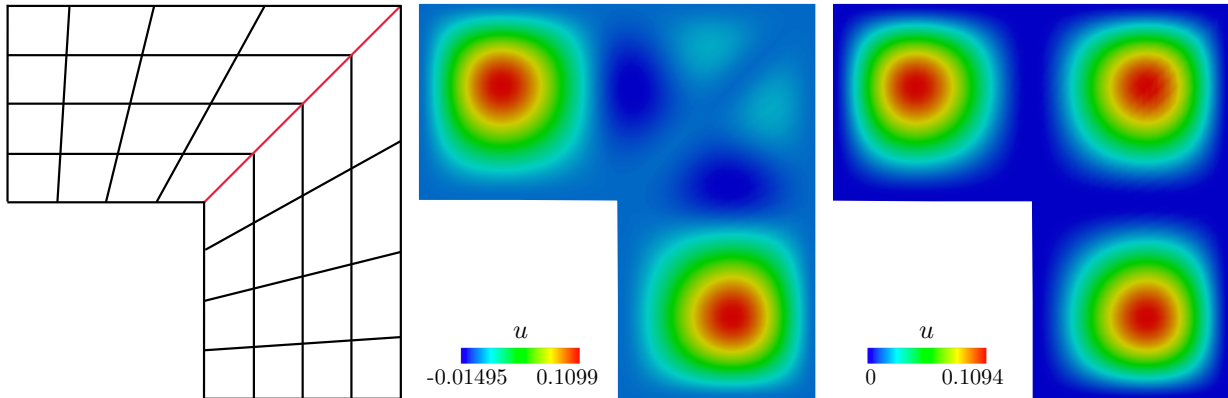


Figure 4: Two-patch L-shaped domain (left), a solution affected by C^1 locking for $p = 3$, $r = 2$ (center), and a correct numerical solution for $p = 3$, $r = 1$ (right).

We start with the L-shaped geometry consisting of two patches. The L-shaped domain is given in Figure 4 (left), where the red edge is the common edge of both patches. Here the parametrization of both patches is bilinear. This is obviously an AS G^1 geometry (recall Proposition 3). Using Theorem 1, the optimal convergence is achieved if and only if $r \leq p-2$ as summarized in Corollary 1. If we focus on degree $p = 3$, C^1 locking is evident when the regularity equals to $r = p - 1 = 2$, see Figure 4 (center). In particular, the solution on the interface line equals to 0. In order to circumvent C^1 locking, we decrease the regularity, see Figure 4 (right). Figure 5 gives the convergence curves for degrees $p = 3, 4$ and 5. We obtain expected results for all degrees, *i.e.* we have convergence (which is optimal) if and only if $r + 2 \leq p$.

8.2.2. Multi-patch geometries (triangle, quarter of a circle and rectangle)

In what follows, we consider cases with three or more patches, starting with an example with three bilinear patches forming a triangle (see Figure 6 (left)) and another with three bi-quadratic patches forming the quarter of a circle (see Figure 7 (left)). Both are AS G^1 geometries. Note that the quarter of the circle is composed of NURBS patches, and is obtained following Section 7 construction, from a geometry parametrization that is an AS G^1 surface in homogeneous coordinates. The details of this construction are presented in the appendix. Figures 6 (center) and 7 (center) show C^1 locking which appears with $p = 3$ and $r = 2$ that we can circumvent by reducing the regularity, see Figures 6 (right) and 7 (right). The expected convergence orders are given in Figure 8.

Next we consider a rectangle composed of four patches, see Figure 9 (left). As shown in this figure, we consider a particular case where two interfaces are collinear. This configuration is among the ones analyzed in [8, Section 11.2.3]. The results are presented in Figure 9 for degree $p = 3$ and regularity $r = 2$ (center) and $r = 1$ (right). Figure 11 (left) gives the convergence orders, which are as expected.

As a final example of analysis-suitable G^1 geometries, we consider a rectangle composed of five

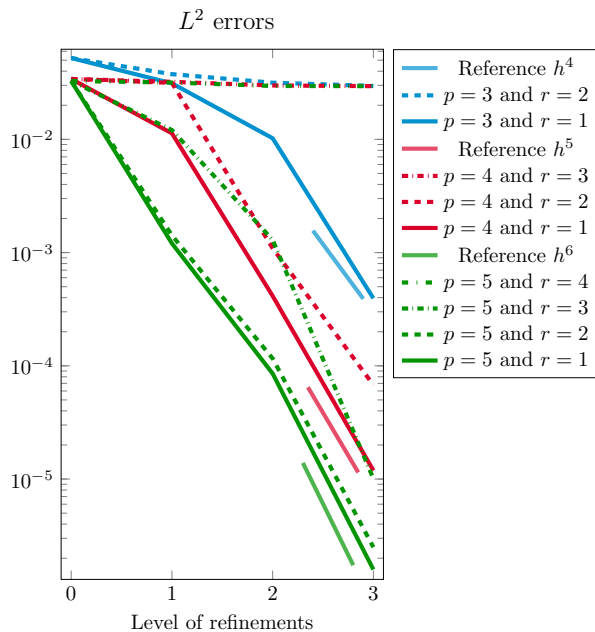


Figure 5: Convergence results for the L-shaped domain.

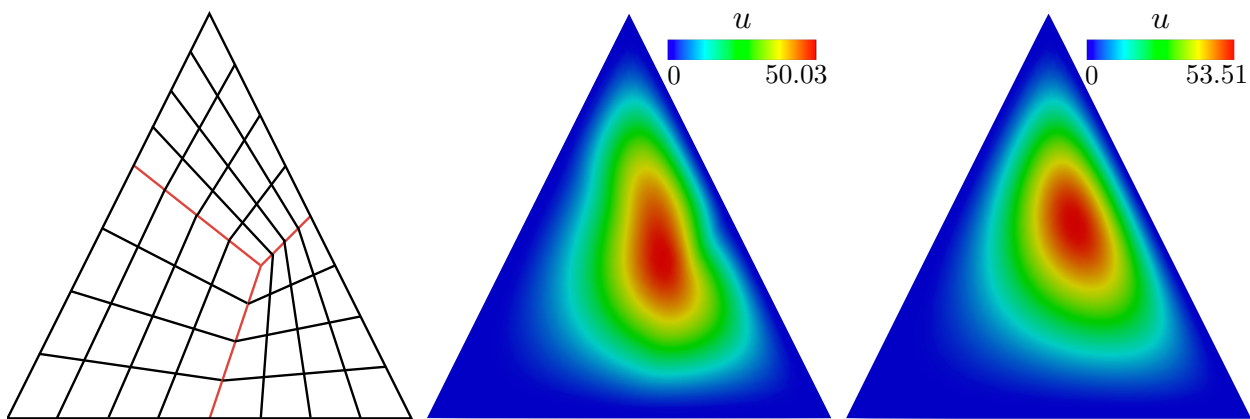


Figure 6: Three-patch triangle (left), a solution affected by C^1 locking for $p = 3$, $r = 2$ (center), and a correct numerical solution for $p = 3$, $r = 1$ (right).

patches, see Figure 10 (left). The results are presented in Figure 10 for degree $p = 3$ and regularity $r = 2$ (center) and $r = 1$ (right). Figure 11 (right) gives the convergence orders, which are again as expected.

8.3. Non-analysis-suitable G^1 geometries

In this section we study two different examples of non-analysis-suitable G^1 geometries. First we consider a two-patch parametrization of a rectangle, where we compare a distorted parametrization with the undistorted identity mapping, see Figure 13. As a second example we consider a five-patch circle.

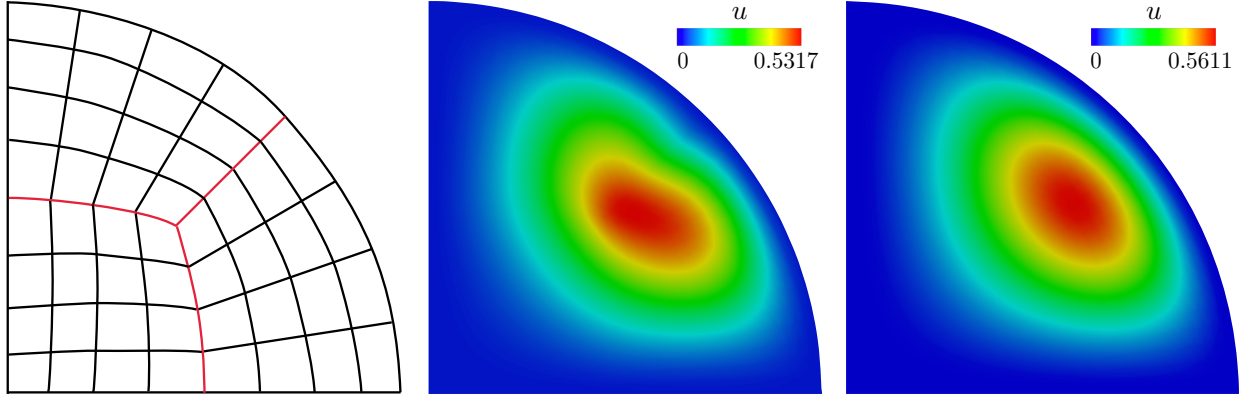


Figure 7: Three-patch quarter of a circle (left), a solution affected by C^1 locking for $p = 3, r = 2$ (center), and a correct numerical solution for $p = 3, r = 1$ (right).

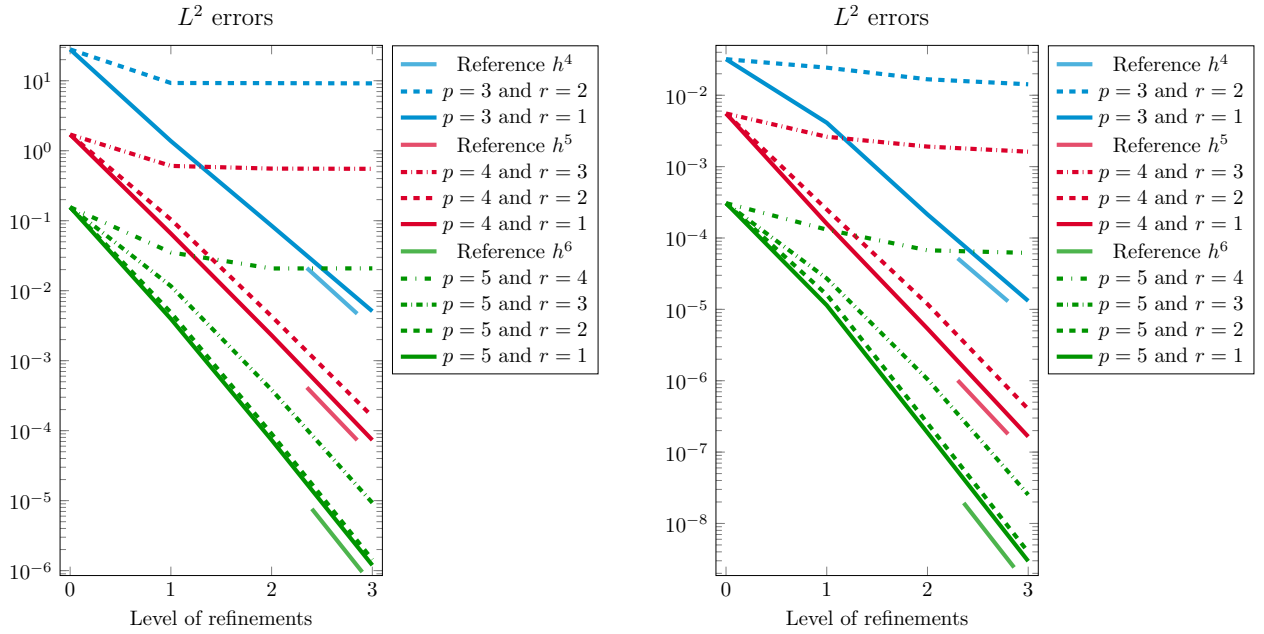


Figure 8: Convergence results for the triangle (left) and the quarter of circle (right).

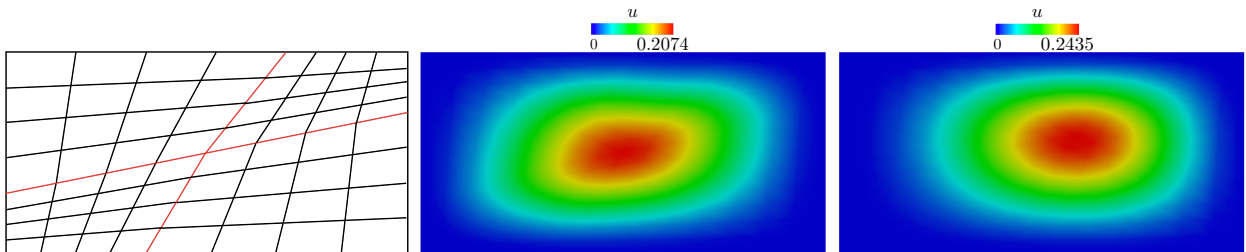


Figure 9: Four-patch rectangle (left), a solution affected by C^1 locking for $p = 3, r = 2$ (center), and a correct numerical solution for $p = 3, r = 1$ (right).

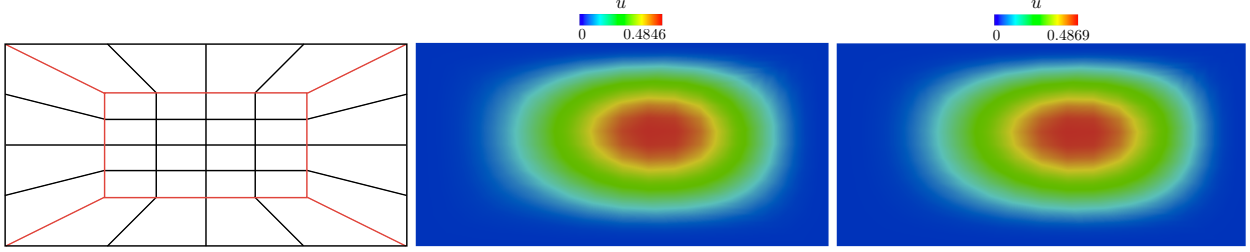


Figure 10: Five-patch rectangle (left), a solution affected by C^1 locking for $p = 3, r = 2$ (center), and a correct numerical solution for $p = 3, r = 1$ (right).

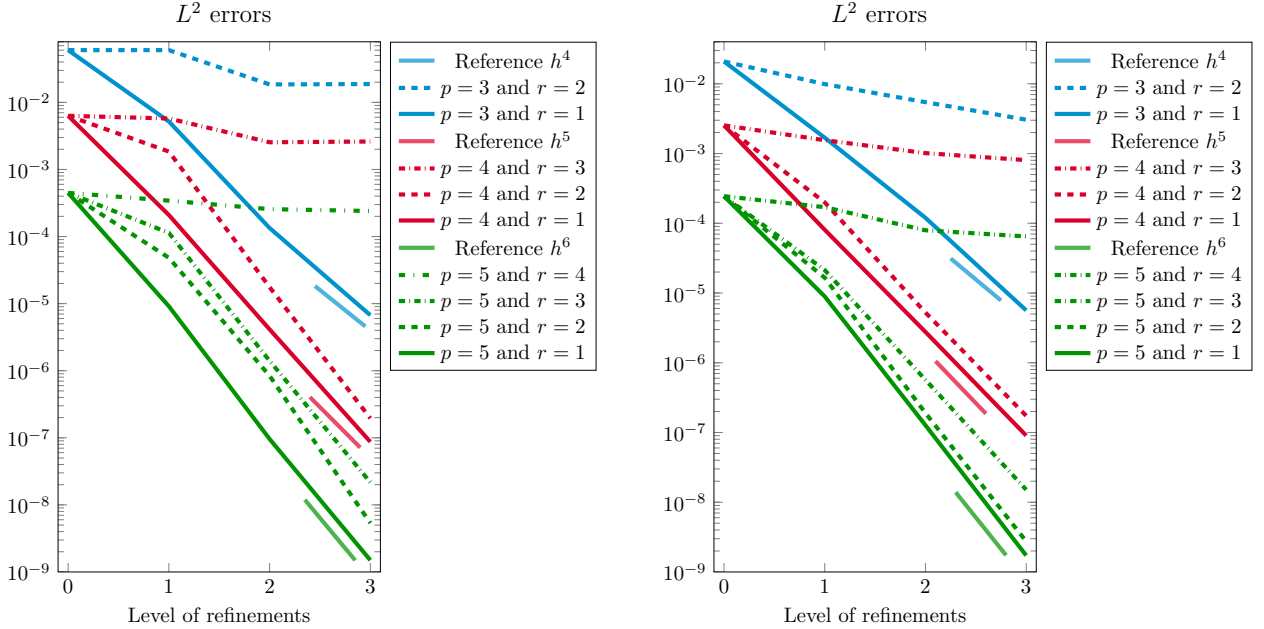


Figure 11: Convergence results for the four-patch rectangle (left) and the five-patch rectangle (right).

8.3.1. Two-patch geometry (quadratically distorted rectangle)

We consider a rectangle domain $[-1, 1] \times [0, 1]$ formed by two patches, where the left one is linear (identity) and right one is quadratic in the horizontal direction and linear in the vertical, see Figure 12 (left). This case illustrates the configuration covered by Theorem 3 and Corollary 2. As shown in Figure 12, with degree $p = 3$, C^1 locking is manifested for both $r = 2$ and $r = 1$, see respectively the second and the third columns of the figure. In order to have convergence, a degree of at least $p = 4$ has to be selected, see Figure 12 (right).

However, as anticipated in Corollary 2, we cannot expect optimal convergence. This is a direct implication of Theorem 3, which for this case ($p_\alpha = 2$ and $\beta^{(R)} = 0$) states that for all $\phi \in \mathcal{V}^1$

$$\left. \frac{\partial \phi}{\partial x} \right|_{\Gamma} \in \mathcal{S}_r^{p-p_\alpha}(\Gamma) = \mathcal{S}_1^2(\Gamma). \quad (54)$$

Assume that the exact solution w is smooth enough and let w_h be the numerical solution. Then, using (54), together with the usual approximation estimates in Sobolev norms and the trace inequality

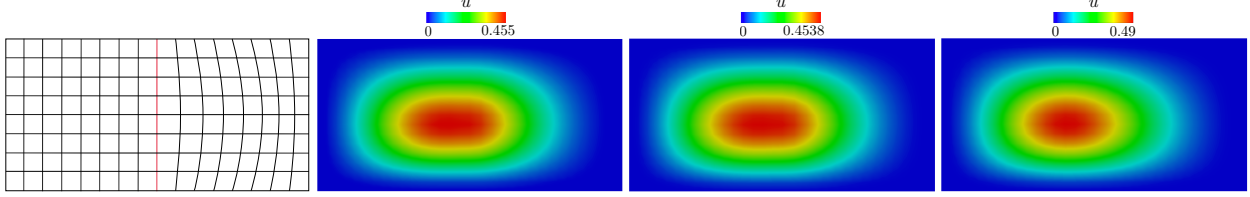


Figure 12: Non-AS G^1 rectangle (left), two solutions affected by C^1 locking for $p = 3$, $r = 2$ (center-left) and $p = 3$, $r = 1$ (center-right), as well as a correct numerical solution for $p = 4$, $r = 1$ (right).

for Sobolev spaces, gives

$$C_{approx} h^{2.5} \simeq \left\| \frac{\partial w}{\partial x} - \frac{\partial w_h}{\partial x} \right\|_{H^{\frac{1}{2}}(\Gamma)} \leq C_{trace} \|w - w_h\|_{H^2(\Omega)},$$

instead of the optimal order of convergence, that is h^3 when measuring the error in the $H^2(\Omega)$ -norm.

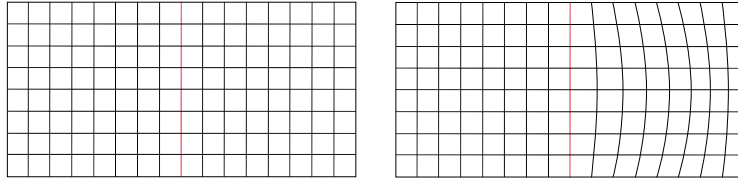


Figure 13: Two-patch rectangle with identity mapping (left), two-patch rectangle with a quadratic distorted patch (right).

In Figure 14 we report the convergence results and, due to the specificity of this case, both L^2 and H^2 norms are plotted. While C^1 locking is easily recognized, from these numerical tests it is difficult to measure the expected sub-optimality of the asymptotic behavior. This is likely a numerical artifact due to the imposition of the C^1 constraint in our implementation, which is discussed in Section 8.4. We further analyze this example in Figure 15, where we compute, for $p = 4$ and $r = 1$, the error only on the left patch, that is $[-1, 0] \times [0, 1]$, and compare the results for this geometry and for a reference geometry formed by the identity mapping on both patches (see Figure 13). Note that on the left patch both parametrizations are the identity mapping.

8.3.2. Multi-patch geometry (circle)

In the last example, we study a circle composed of five patches, given in Figure 16 (left). This is an alternative to the standard single-patch parametrizations of the circle that are singular. The given parametrization is rational. However, it does not fit into the framework presented in the appendix, since the homogeneous representation is not an analysis-suitable G^1 surface. Therefore it is beyond our previous study. However, the results obtained here are consistent with our findings. For degree $p = 3$ the numerical solution suffers of C^1 locking, as one can see in Figure 16 for regularity $r = 2$ (center-left) and $r = 1$ (center-right). For degree $p = 4$ and regularity $r = 1$, see Figure 16 (right), we observe convergence to a solution. Figure 17 (right) gives the convergence behavior for degrees $p = 3, 4$ and 5. Sub-optimality in all situations is manifested.

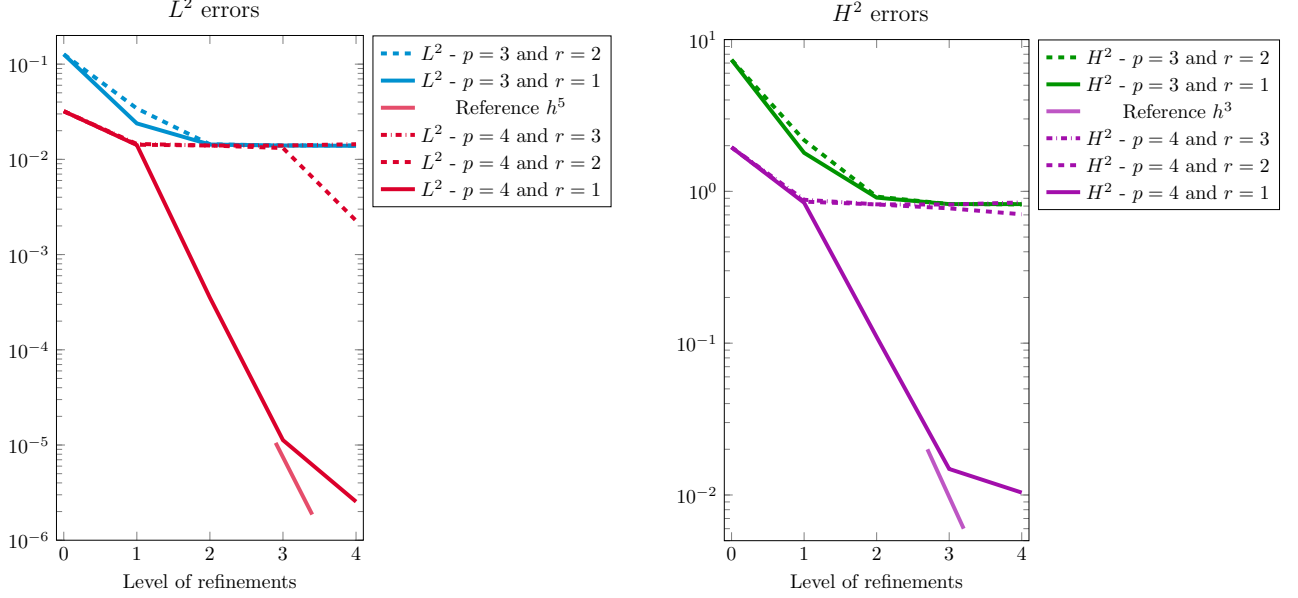


Figure 14: Convergence results for the non-AS G^1 two-patch rectangle, with error in L^2 (left) and H^2 (right).

8.4. Numerical implementation of C^1 continuity

In this section, we describe the numerical implementation of C^1 continuity that we have used in order to obtain all the numerical examples given previously. Let A and b , be the matrix and the right and side of the system corresponding to the variational formulation (53), where no boundary condition or continuity condition are included. Furthermore, let C_1 be the C^1 constraint matrix in symmetric form, i.e.

$$(C_1)_{i,j} = \int_{\Gamma} (\vec{\nabla} \phi_i \cdot \vec{n}) (\vec{\nabla} \phi_j \cdot \vec{n}).$$

Let N_0 be the change of basis matrix from the fully unconstrained space to the subspace fulfilling boundary condition and C^0 continuity. N_0 can be seen as obtained from the identity $I_{N_{unc}}$ – where N_{unc} is the number of degrees of freedom without constraints – by removing the columns with index corresponding to the degrees of freedom of the boundary conditions and by summing the columns of degrees of freedom that are shared on Γ . Since it is not trivial to compute a C^1 continuous basis analytically, we operate numerically by computing the null-space

$$N_1 = \text{null}(N_0^T C_1 N_0). \quad (55)$$

Then we solve the following problem: find z such that

$$N_1^T N_0^T A N_0 N_1 z = N_1^T N_0^T b, \quad (56)$$

and obtain the solution in the unconstrained initial spline basis as $x = N_0 N_1 z$.

The numerical computation of (55) is a hard task for non AS G^1 geometries. Indeed, the non-zero eigenvalues of $N_0^T C_1 N_0$ are not well separated from the null eigenvalues as shown in Figure 18

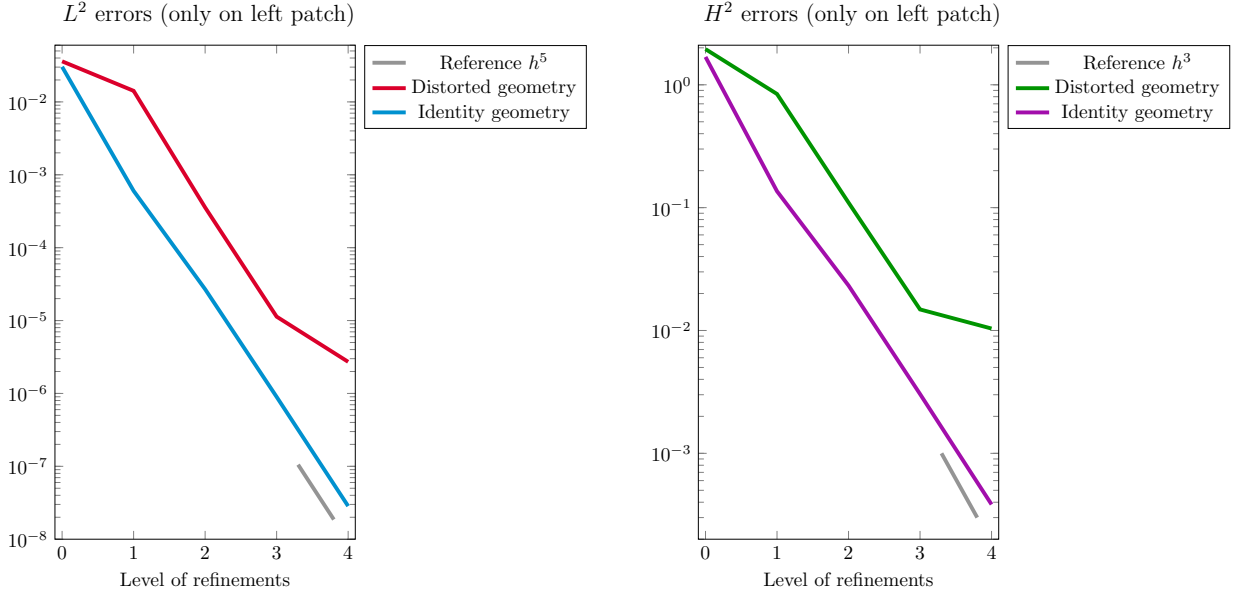


Figure 15: Comparison of convergence between the two geometries given in Figure 13 for $p = 4$ and $r = 1$; the error is computed only in the left subdomain $[-1, 0] \times [0, 1]$ in L^2 (left plot) and H^2 (right plot).

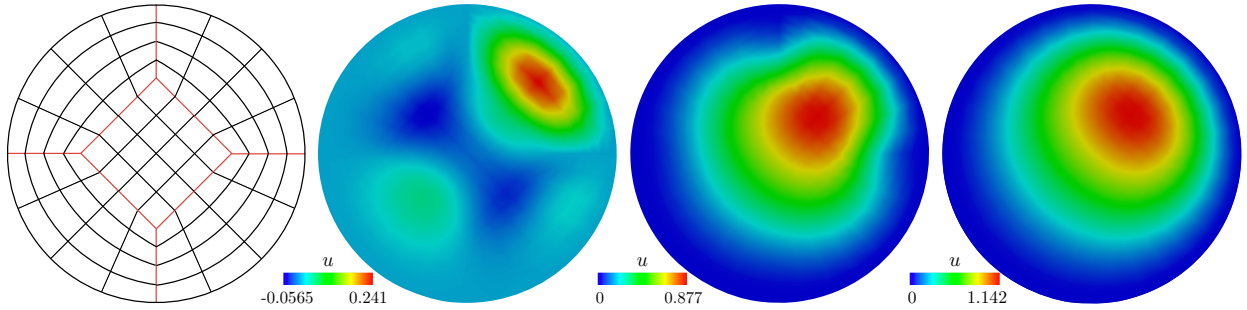


Figure 16: Five-patch circle (left), two solutions affected by C^1 locking for $p = 3, r = 2$ (center-left) and for $p = 3, r = 1$ (center-right), as well as a correct numerical solution for $p = 4, r = 1$ (right).

for the distorted rectangular domain in Figure 12 (left), with $p = 4, r = 1$. By comparison, Figure 19 shows the eigenvalues for the L-shaped domain with the same degree and regularity. The two configurations are structurally equivalent, i.e. the topology of the control point grid is the same.

9. Conclusions

In this paper, we study C^1 -smooth isogeometric function spaces over multi-patch geometries. In this context, we consider geometry parametrizations composed of multiple patches that meet C^0 at patch interfaces. As it was already shown in [20] an isogeometric function over such a domain is C^1 if and only if its graph surface parametrization is G^1 . In the framework, we consider that the geometry parametrization is given initially and fixed. From that, the geometric continuity

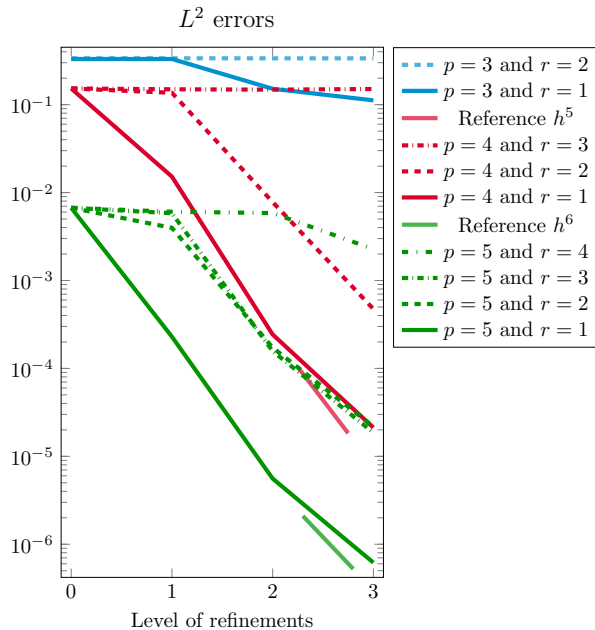


Figure 17: Convergence results for the five-patch circle.

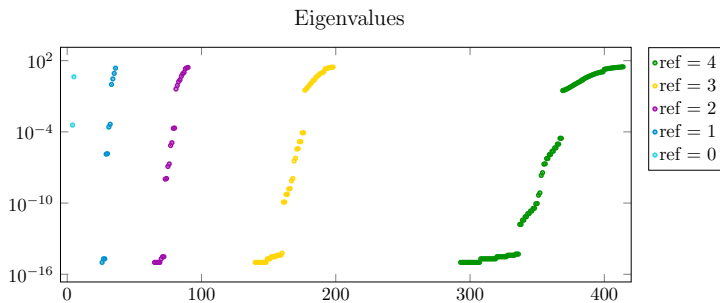


Figure 18: Eigenvalues of the domain given in Figure 12 (left) for $p = 4$ and $r = 1$, and different h -refinement levels.

conditions are derived. The same conditions need to be satisfied for the graph parametrizations of the isogeometric functions in order to obtain a C^1 -smooth function space over the given geometry.

We study how these conditions affect the traces and the normal derivatives of the isogeometric function spaces along the patch interfaces. If the trace or normal derivative along the interface is over-constrained, the approximation order of the isogeometric function space is reduced. We identify a class of configurations that allows for optimal approximation properties of C^1 isogeometric spaces, so called *analysis-suitable G^1* (AS G^1) geometry parametrizations. We show that AS G^1 geometries indeed allow for optimal approximation. Moreover, parametrizations that are not AS G^1 suffer from C^1 locking, i.e. the order of approximation is reduced. In the worst case the convergence under h -refinement is prohibited due to full C^1 locking.

We develop all the theoretical results for planar B-spline geometries and present generalizations to surfaces and NURBS patches. All the results are supported and confirmed by numerical tests

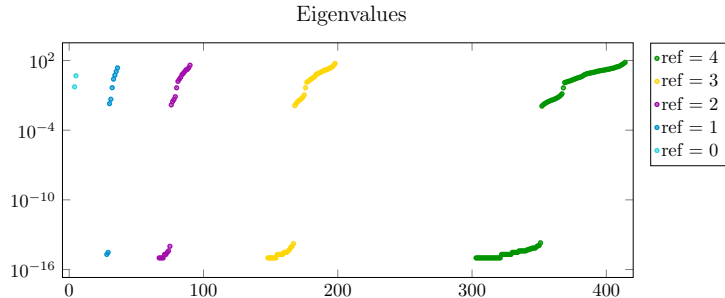


Figure 19: Eigenvalues of the L-shaped domain given in Figure 4 (left) for $p = 4$ and $r = 1$, and different h -refinement levels.

for various degrees and orders of regularity of the spline space. We numerically solve a bilaplacian problem over several analysis-suitable and non-analysis-suitable geometries using a standard Galerkin approach. As we pointed out, the numerical implementation of the C^1 conditions poses some non-negligible difficulties for complex configurations of non-analysis-suitable geometries.

An important question that remains to be studied in more detail is the flexibility of analysis-suitable G^1 geometries. As we have shown, AS G^1 contains bilinear patches but extends to more general configurations. We formulate the problem of flexibility in the following way – Given a collection of boundary curves, is it possible to find patches that interpolate the boundary curves and that form an AS G^1 geometry? – This question of flexibility may depend strongly on the given degree of the boundary curves and on the degree of the B-spline patches. For piecewise linear boundary curves, the problem can be solved by using bilinear patches. An extension to higher degrees is however not straight-forward and requires further investigation.

Acknowledgments

The authors would like to thank Pablo Antolin and Massimiliano Martinelli for fruitful discussions on the topics of the paper. The authors were partially supported by the European Research Council through the FP7 Ideas Starting Grant *HIGEOM*. This support is gratefully acknowledged.

Appendix: AS G^1 parametrization of a quarter of circle

In this appendix we discuss in detail the construction of the geometry parametrization of the example shown in Figure 7 in Section 8.2.2. This is based on the NURBS setting of Section 7 and on the ideas in [8] as well as [20, Section 3.4]. Each patch of the three-patch geometry is constructed from a combination of a bilinear mapping

$$\mathbf{B}^{(i)} : [0, 1]^2 \rightarrow Q^{(i)} \subset \Delta = \{(u, v) \in [0, 1]^2 : u + v \leq 1\}$$

onto a quadrilateral $Q^{(i)}$ within a reference triangle Δ and a global mapping

$$\tilde{\mathbf{G}} : \Delta \rightarrow \tilde{\Omega} \subset \mathbb{R}^3$$

from the reference triangle to the surface patch $\tilde{\Omega}$ in homogeneous coordinates. These mappings and corresponding domains are shown in Figure 20.

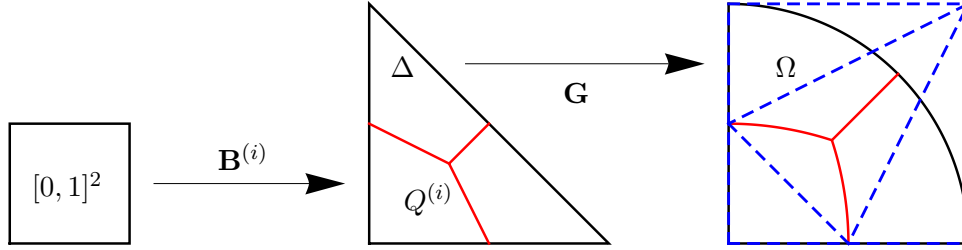


Figure 20: Mappings $\mathbf{B}^{(i)}$ and \mathbf{G} and corresponding domains.

Here the mapping $\tilde{\mathbf{G}}$ is a triangular Bézier patch of total degree $p = 2$ with

$$\tilde{\mathbf{G}}(s, t) = \sum_{i+j+k=2} g_{i,j,k} s^i t^j (1-s-t)^k \frac{i! j! k!}{2},$$

with control points

$$\begin{aligned} g_{0,0,2} &= (0, 0, 1)^T & g_{0,1,1} &= (0, \sqrt{2}, 2\sqrt{2})^T & g_{0,2,0} &= (0, 1, 1)^T \\ g_{1,0,1} &= (\sqrt{2}, 0, 2\sqrt{2})^T & g_{1,1,0} &= (2\sqrt{2}, 2\sqrt{2}, 2\sqrt{2})^T \\ g_{2,0,0} &= (1, 0, 1)^T \end{aligned}$$

in homogeneous coordinates. In Figure 20, the dashed blue lines represent the corresponding control point grids in Cartesian coordinates. Each quadrilateral $Q^{(1)}$, $Q^{(2)}$ and $Q^{(3)}$ is formed by one corner point of the triangle Δ , two adjacent edge midpoints as well as the center of gravity $(1/3, 1/3)^T$. The bilinear mapping $\mathbf{B}^{(i)}$ is (up to rotations of the parameter domain) completely determined by its image $Q^{(i)}$. By construction, the mapping $\mathbf{F}^{(i)} = \mathbf{G} \circ \mathbf{B}^{(i)}$ is a rational bi-quadratic function in each component.

Using this construction, the theory developed in Sections 6 and 7 can be applied to the example in Figure 7.

References

- [1] Y. Bazilevs, L. Beirao da Veiga, J. A. Cottrell, T. JR Hughes, and G. Sangalli. Isogeometric analysis: approximation, stability and error estimates for h-refined meshes. *Mathematical Models and Methods in Applied Sciences*, 16(07):1031–1090, 2006.
- [2] E. Beeker. Smoothing of shapes designed with free-form surfaces. *Computer-aided design*, 18(4):224–232, 1986.
- [3] L. Beirao da Veiga, A. Buffa, C. Lovadina, M. Martinelli, and G. Sangalli. An isogeometric method for the Reissner–Mindlin plate bending problem. *Computer Methods in Applied Mechanics and Engineering*, 209:45–53, 2012.

- [4] L. Beirao da Veiga, A. Buffa, J. Rivas, and G. Sangalli. Some estimates for h–p–k-refinement in isogeometric analysis. *Numerische Mathematik*, 118(2):271–305, 2011.
- [5] L. Beirao Da Veiga, A. Buffa, G. Sangalli, and R. Vázquez. Mathematical analysis of variational isogeometric methods. *Acta Numerica*, 23:157–287, 2014.
- [6] L. Beirao Da Veiga, D. Cho, and G. Sangalli. Anisotropic NURBS approximation in isogeometric analysis. *Computer Methods in Applied Mechanics and Engineering*, 209:1–11, 2012.
- [7] D. J. Benson, Y. Bazilevs, M.-C. Hsu, and T. JR Hughes. A large deformation, rotation-free, isogeometric shell. *Computer Methods in Applied Mechanics and Engineering*, 200(13):1367–1378, 2011.
- [8] M. Bercovier and T. Matskewich. Smooth Bezier surfaces over arbitrary quadrilateral meshes. *arXiv preprint arXiv:1412.1125*, 2014.
- [9] E. Brivadis, A. Buffa, B. Wohlmuth, and L. Wunderlich. Isogeometric mortar methods. *Computer Methods in Applied Mechanics and Engineering*, 284:292–319, 2015.
- [10] F. Buchegger, B. Jüttler, and A. Mantzaflaris. Adaptively refined multi-patch B-splines with enhanced smoothness. *Applied Mathematics and Computation*, page in press, 2015.
- [11] F. Cirak, M. J. Scott, E. K. Antonsson, M. Ortiz, and P. Schröder. Integrated modeling, finite-element analysis, and engineering design for thin-shell structures using subdivision. *Computer-Aided Design*, 34(2):137–148, 2002.
- [12] J. A. Cottrell, T. JR Hughes, and Y. Bazilevs. *Isogeometric analysis: toward integration of CAD and FEA*. Wiley, 2009.
- [13] J. A. Evans, Y. Bazilevs, I. Babuška, and T. JR Hughes. n-Widths, sup–infs, and optimality ratios for the k-version of the isogeometric finite element method. *Computer Methods in Applied Mechanics and Engineering*, 198(21):1726–1741, 2009.
- [14] H. Gómez, V. M Calo, Y. Bazilevs, and T. JR Hughes. Isogeometric analysis of the Cahn–Hilliard phase-field model. *Computer Methods in Applied Mechanics and Engineering*, 197(49):4333–4352, 2008.
- [15] H. Gómez, T. JR Hughes, X. Nogueira, and V. M. Calo. Isogeometric analysis of the isothermal Navier–Stokes–Korteweg equations. *Computer Methods in Applied Mechanics and Engineering*, 199(25):1828–1840, 2010.
- [16] D. Groisser and J. Peters. Matched G^k -constructions always yield C^k -continuous isogeometric elements. *Computer aided geometric design*, 34:67–72, 2015.
- [17] T. JR Hughes, J. A. Cottrell, and Y. Bazilevs. Isogeometric analysis: CAD, finite elements, NURBS, exact geometry and mesh refinement. *Computer methods in applied mechanics and engineering*, 194(39):4135–4195, 2005.

- [18] T. JR Hughes, A. Reali, and G. Sangalli. Duality and unified analysis of discrete approximations in structural dynamics and wave propagation: comparison of p-method finite elements with k-method NURBS. *Computer methods in applied mechanics and engineering*, 197(49):4104–4124, 2008.
- [19] B. Jüttler, A. Mantzaflaris, R. Perl, and M. Rumpf. On isogeometric subdivision methods for PDEs on surfaces. 2015.
- [20] M. Kapl, V. Vitrih, B. Jüttler, and K. Birner. Isogeometric analysis with geometrically continuous functions on two-patch geometries. *submitted*, 2015.
- [21] J. Kiendl, K.-U. Bletzinger, J. Linhard, and R. Wüchner. Isogeometric shell analysis with Kirchhoff-Love elements. *Computer Methods in Applied Mechanics and Engineering*, 198(49):3902–3914, 2009.
- [22] S. K. Kleiss, C. Pechstein, B. Jüttler, and S. Tomar. IETI - isogeometric tearing and interconnecting. *Computer Methods in Applied Mechanics and Engineering*, 247-248(0):201 – 215, 2012.
- [23] D Liu and J Hoschek. G^1 continuity conditions between adjacent rectangular and triangular Bézier surface patches. *Computer-Aided Design*, 21(4):194–200, 1989.
- [24] T. Lyche and G. Muntingh. A Hermite interpolatory subdivision scheme for C^2 -quintics on the Powell–Sabin 12-split. *Computer Aided Geometric Design*, 31(7):464–474, 2014.
- [25] T. Nguyen, K. Karčiauskas, and J. Peters. A comparative study of several classical, discrete differential and isogeometric methods for solving Poisson’s equation on the disk. *Axioms*, 3(2):280–299, 2014.
- [26] M. S. Pauletti, M. Martinelli, N. Cavallini, and P. Antolin. Iगतools: An Isogeometric Analysis Library. *SIAM Journal on Scientific Computing*, 2015.
- [27] J. Peters. Smooth interpolation of a mesh of curves. *Constructive Approximation*, 7(1):221–246, 1991.
- [28] G. Sangalli, T. Takacs, and R. Vázquez. Unstructured spline spaces for isogeometric analysis based on spline manifolds. *arXiv preprint arXiv:1507.08477*, 2015.
- [29] M. A. Scott, R. N. Simpson, J. A. Evans, S. Lipton, S. P. A. Bordas, T. JR Hughes, and T. W. Sederberg. Isogeometric boundary element analysis using unstructured T-splines. *Computer Methods in Applied Mechanics and Engineering*, 254:197–221, 2013.
- [30] M. A. Scott, D. C. Thomas, and E. J. Evans. Isogeometric spline forests. *Computer Methods in Applied Mechanics and Engineering*, 269:222–264, 2014.

- [31] H. Speleers, C. Manni, F. Pelosi, and M. L. Sampoli. Isogeometric analysis with Powell–Sabin splines for advection–diffusion–reaction problems. *Computer Methods in Applied Mechanics and Engineering*, 221:132–148, 2012.
- [32] S. Takacs and T. Takacs. Approximation error estimates and inverse inequalities for B-splines of maximum smoothness. *arXiv preprint arXiv:1502.03733*, 2015.
- [33] T. Takacs, B. Jüttler, and O. Scherzer. Derivatives of isogeometric functions on n-dimensional rational patches in R^d . *Computer Aided Geometric Design*, 31(7-8):567 – 581, 2014. Recent Trends in Theoretical and Applied Geometry.